

TECTONIC-SEDIMENTARY INTERPLAY, OUACHITA MOUNTAINS

TECTONIC-SEDIMENTARY INTERPLAY OF A MULTI-SOURCED,
STRUCTURALLY-CONFINED DEEPWATER SYSTEM IN A FORELAND BASIN
SETTING: THE PENNSYLVANIAN LOWER ATOKA FORMATION,
OUACHITA MOUNTAINS, USA

Pengfei Hou*, Lesli J. Wood, Zane R. Jobe

Department of Geology and Geological Engineering, Colorado School of Mines

* Corresponding author, Email: pengfei.hou@outlook.com

ABSTRACT

Submarine fans deposited in structurally complex settings record important information on basin evolution and tectonic-sedimentary relationships but are often poorly preserved in outcrops due to post-depositional deformation. This study integrates both new field data as well as data compiled from literature to demonstrate the spatial facies variability of the deep-water lower Atoka formation (Lower Pennsylvanian) that occupies a structurally complex early foreland-basin setting. The lower Atoka outcrops in the Ouachita Mountains and the southern Arkoma Basin in the USA are divided into three structural-depositional zones: foredeep, wedge-top, and foreland. Although the mean paleoflow is axial, each zone exhibits unique patterns in facies distribution. The foredeep consists of a large westward-prograding fan and a small eastward-prograding fan on the western part and exhibits significant longitudinal and lateral facies changes. The wedge-top consists of a westward-prograding fan and exhibits subtle longitudinal facies change. The foreland consists of small slope channel and fan systems along the northern and western margins. We interpret the characteristics of facies distributions in the three zones as the result of different combinations of lateral structural-topographic confinement, sediment supply, and paleogeographic locations. This study provides an improved understanding of the lower Atoka deepwater system and has implications for the tectonic-sedimentation relationship on the southern Laurentia continental margin during the Ouachita Orogeny.

INTRODUCTION

Understanding the interactions of turbidity currents with structurally complex substrates is increasingly important with increasing hydrocarbon exploration and development in basins with complex seafloor bathymetry, such as deepwater fold and thrust

belts, rift basins, and foreland basin systems (Ravnås and Steel, 1998; Gawthorpe and Leeder, 2000; Mutti et al., 2003; Morley et al., 2011; DeCelles, 2012). Such depositional systems also preserve important information on basin evolution, tectonic histories of continental margins, and paleoclimate (Hatcher et al., 1989; Stow and Tabrez, 2002; Allen and Allen, 2005; Hessler and Fildani, 2019). Syn-depositional tectonics can influence deepwater sedimentation by modifying accommodation, diverging sediment transport, inducing flow transformations, or inducing changes in sediment supply (Vinnels et al., 2010; DeCelles, 2012; Salles et al., 2014; Jobe et al., 2015; Wang et al., 2017). Outcrop studies on ancient foreland basins provide numerous examples to explore this turbidite-tectonic relationship. For example, syn-depositional thrust faults and induced topographic highs can cause flow confinement or basin segmentation in either foredeep or wedge-top depozones (Felletti, 2002; Mutti et al., 2009; Tinterri et al., 2017). Breaching of topographic barriers provides connections between different basin segments that result in complex sediment dispersal patterns (Lomas and Joseph, 2004; Salles et al., 2014; Burgreen and Graham, 2014). However, interpreting these relationships can be challenging due to post-depositional deformation and erosion (Pinter et al., 2016, 2018). How to best utilize the fragmented stratigraphic records to extract maximum information of the depositional system remains a key question. We chose the deepwater succession of the lower member of the Pennsylvanian Atoka Formation in the Ouachita Mountains to address this question.

The Atoka Formation is a sedimentary record of the Carboniferous-late phase transition of the Laurentia continent from a passive to an active margin (Stark, 1966; Cline, 1968; Briggs, 1974; Houseknecht, 1986; Haley et al., 1993). The lower Atoka has been interpreted as a laterally-confined, fined-grained deepwater system (Morris, 1974b; Graham et al., 1975; Sprague, 1985; Coleman, 2000). However, there is a lack of basin-wide investigation on the relationship of deepwater deposition and this Carboniferous-age

structural evolution in the Ouachita Mountains. The purpose of this study is to (a) quantitatively document the patterns of facies distribution of the lower Atoka sediment-gravity-flow deposits, and (b) investigate the tectonic-sedimentary relationship using a refined understanding of deepwater depositional systems and regional structural history.

GEOLOGIC SETTING

Tectonic setting and structural framework

The Ouachita Mountains and southern Arkoma Basin cover an area of 400 by 150 km² in Arkansas and Oklahoma, USA (Fig. 1). The Ouachita Mountains are the largest exposures of the Paleozoic Ouachita Fold and Thrust Belt (OFTB, Mickus and Keller, 1992), which is genetically related to the Appalachian Orogen to the northeast and the Marathon Orogen to the southwest (Thomas, 2004, 2011). The collision of Laurentia and Gondwana created this chain of foreland basins (Hatcher et al., 1989). During the mid-Carboniferous, the study area evolved from a remnant ocean basin (Ouachita trough) into a foreland basin (Arkoma Basin) (Houseknecht, 1986; Mickus and Keller, 1992; Keller and Hatcher, 1999), with an estimated amount of shortening of 50% (Coleman, 2000). Meanwhile, rapid subsidence and abundant sediment supply resulted in a thick turbidite succession being deposited from Late Mississippian to Middle Pennsylvanian (Thomas, 1976; Houseknecht, 1986). In this study, we informally termed the genetically-related Ouachita Mountains and the southern Arkoma Basin combined as the Greater Arkoma Basin (GAB) (*sensu* 'Arkoma Basin Province', Perry, 1995; Houseknecht et al., 2010).

The GAB has been divided into several zones (Figs. 1 & 2) based on structural and sedimentological characteristics (Arbenz, 1989, 2008; Haley and Stone, 1994). We simplified the scheme of Arbenz (2008) and divided the study area into three zones from north to south,

namely the southern foreland, foredeep, and wedge-top, which are separated by the Ross Creek-Choctaw faults and the Y City-Ti Valley faults, respectively. The main structural strike of these faults, as well as these provinces, are east-west in Arkansas and northeast-southwest in Oklahoma (Haley et al., 1993; Arbenz, 2008). The wedge-top (Ouachita Allochthon) is the main part of the Ouachita Mountains and presumably has a large areal extent buried beneath the Cretaceous coastal plain deposits (Nelson et al., 1982; Lillie et al., 1983; Mickus and Keller, 1992). The largest structures in the wedge-top are the Benton Uplift in Arkansas and the Broken Bow Uplift in Oklahoma (BU-BBU), which are basement-involved anticlinoriums that form the core of the Ouachita Mountains (Viele, 1966).

The foredeep and wedge-top have important along-strike variations in structural styles (Thomas, 2004; Arbenz, 2008). In the foredeep, the eastern part is characterized by thick and competent strata, large folds (e.g. the Fourche La Fave Syncline), large triangle zones (Arbenz, 2008), and less shortening (Harry and Mickus, 1998). In contrast, the western part is characterized by thin and incompetent strata, small folds, small triangle zones, imbricated thrust faults (Arbenz, 2008), and more shortening (Harry and Mickus, 1998). Northeastern portions of the wedge-top (Maumelle Chaotic Zone) are characterized by intense syn- and post-depositional deformation (Viele, 1966, 1979; Morris, 1971a; Viele and Thomas, 1989). In contrast, western portions of the wedge-top are characterized by broad synclines (e.g. Lynn Mountain and Boktukola synclines), tightly-folded and faulted anticlines, a small imbricate zone, and uplift (Potato Hills) in the north (Haley et al., 1993; Arbenz, 2008). The development of the main structures is episodic and largely synchronous with foreland deposition during the Late Mississippian-Middle Pennsylvanian (Arne, 1992; Babaei and Viele, 1992; Arbenz, 2008; Johnson, 2011; Shaulis et al., 2012).

History of deposition

During the Cambrian-Middle Mississippian, the GAB was characteristic of a passive continental margin. The basin fill consists of ~4000 m of deep marine shale, chert, and turbidite, the mean depositional rate of which is 30 m/Myr. The shelf equivalent is characterized by carbonate platform deposition (Morris, 1974b). During the Middle Mississippian-Middle Pennsylvanian, the GAB was characteristic of an active margin. The basin filled with a thick succession (>10 km) of sediment-gravity-flow deposits, namely the Stanley Group, Jackfork Group, Johns Valley Formation, and the lower part of the Atoka Formation, at an average depositional rate of 300 m/Myr (Morris, 1974a). The remainder of the Atoka Formation is a shoaling upward succession ranging from slope fan to deltaic and shallow marine deposits (Zachry and Sutherland, 1984; Houseknecht, 1986; Haley et al., 1993). The approximate duration of the entire Atoka Formation is 5 Myr (Davydov et al., 2010). During the Middle Pennsylvanian, the GAB transitioned into a continental foreland basin filled with 100-2500 m of fluvial-deltaic deposits, known as the Krebs Group (Oakes, 1953; Rieke and Kirr, 1984).

This study focuses on the lower Atoka, the typical thickness of which is 600 m, 2000 m, 1500 m in the southern foreland, foredeep, and wedge-top, respectively (Legg et al., 1990; Saleh, 2004; Haley and Stone, 2006; Arbenz, 2008; Godo et al., 2014). The lower Atoka has been interpreted as a delta-fed, multi-sourced, fine-grained submarine fan system (Fig. 3), confined in a narrow and elongated deep-marine basin (Sprague, 1985; Houseknecht, 1986; Coleman, 2000). The estimated basin size during deposition is 550 by 300 km² (Coleman, 2000). The predominant sediment transport direction is axial, from east to west (Morris, 1974b; Sprague, 1985; Ferguson and Suneson, 1988; Gleason, 1994). Additionally, minor sediment sources from the north, west, and south/southeast may have also contributed to the basin (Houseknecht, 1986; Ferguson and Suneson, 1988; Thomas, 1997; Sharrah, 2006). A water depth of 1500-2000 m was estimated for the basin center (Coleman, 2000) and ~200 m

for the slope facies in the southern foreland (Houseknecht, 1986). The submarine fan system in the foredeep consists of a main axial fan in the foredeep and possibly smaller lateral fan system(s) on the northern flank (Houseknecht, 1986); the fan system in the wedge-top zone is poorly documented.

DATASET AND METHODOLOGY

The dataset of this study consists of detailed measured sections from the field and literature. The field dataset includes 35 measured sections of well-exposed outcrops and qualitative observations of less well-exposed outcrops throughout the study area. The measurements recorded the bed-by-bed lithology, sedimentary structures, and trace fossils at 2-cm resolution. Sandstone amalgamation surfaces were carefully identified by grain size changes, differential weathering, and the presence of thin and discontinuous mudstones. No attempt was made to separate turbidite mudstones and hemipelagic mudstones (*sensu* Sylvester, 2007), because true hemipelagic mudstones are difficult to identify, and most of the mudstones are rich in silt and sand (Clark et al., 1999, 2000). The literature-derived dataset includes 19 sections (Chamberlain, 1971; Fulton, 1985; Sprague, 1985) and a summary of qualitative observations from other publications (Table 1; also Supplementary Data). We interpreted all measured sections with a consistent facies scheme. The integrated dataset includes 54 measured sections, 589 paleocurrent readings from flute casts, a total stratigraphic thickness of 2,515 m, and 11,117 individual beds (see Supplementary Data). Hybrid-event beds (Houghton et al., 2003, 2009) and chaotically bedded mass-transport deposits (Moscardelli and Wood, 2015) are rare (<5% by thickness).

Many outcrops are found in clusters of exposures separated by covered intervals within a same thrust sheet. Each cluster is treated as one 'composite section' (Fig. 4). Thus,

we grouped the 54 individual measured sections into 18 composite sections, denoted as S1-S18 (Fig. 4, Supplementary Data). Basin-wide correlations between measured sections are difficult due to lack of recognizable datum and structural complexity (Fulton, 1985; Sprague, 1985; LaGrange, 2002), although short-distance correlation is possible (*sensu* Al-Siyabi, 1998; Sgavetti, 1991; Slatt et al., 2000). We did not attempt to correlate composite sections directly but rather treated each composite section as a sample along the sediment routing system within each structural-depositional zone (Fig. 4). For each composite section, we compiled the facies compositions, paleocurrent patterns, percent sandstone (total sandstone bed thickness over the interval thickness), amalgamation ratio (*sensu* Romans et al., 2009), and the standard deviation of sandstone bed thickness (*sensu* Hansen et al., 2017) to capture the spatial variation of the depositional system. We acknowledge that covered or unsampled intervals in composite sections may influence these metrics, but incomplete exposure prevents full characterization.

RESULTS

Definitions of facies scheme

The facies scheme in this study consists of six types of beds, five types of lithofacies, and four types of facies associations in ascending hierarchical order. A hierarchical approach is useful for studying depositional systems at different scales (Hubbard et al., 2008; Pr lat et al., 2009; Romans et al., 2011). Beds are the deposits of individual turbidity events (Middleton and Hampton, 1973; Normark et al., 1993; Fryer and Jobe, 2019). We defined four types of sandstone beds using lithology, thickness (Pickering and Hiscott, 2016) and sedimentary structures (Table 2), one type of mudstone (which may be composed of multiple events), and one type of chaotic, disturbed event-bed (Table 2).

Lithofacies represent the groupings of beds. The lithofacies scheme in this study is derived from previous schemes for the lower Atoka (Sprague, 1985; Fulton, 1985; LaGrange, 2002) and the analogous Jackfork Group (Morris, 1971b, 1974a; Al-Siyabi, 2000; Slatt et al., 2000; Zou et al., 2012), which are based on classical facies models of siliciclastic deepwater systems (Bouma, 1962; Mutti and Ricci-Lucchi, 1978; Walker, 1978; Mutti, 1985; Bouma, 2000). The scheme consists of five lithofacies denoted as F1 to F5 (Fig. 5). The definitions are given in Table 3 and brief descriptions are as follows: F1. Massive, amalgamated sandstone, which consists primarily of bed types B1 and B2, often occurs at more proximal, channelized, or confined settings. Conglomeratic beds only occur in two localities (Table 1): the basal Atoka in Lynn Mountain Syncline (between S16-S18 in Fig. 4) in Oklahoma (Pauli, 1994) and Eagle Gap in Arkansas (northwest of S10 in Table 1) (Nally, 1996). F2. Thick-bedded sandstone with minor mudstone, which consists primarily of B2 and B3, and the sandstone beds are often graded and structured. F3. Thin-bedded sandstone and mudstone, consisting primarily of B3 and B4 with no more than 50% mudstone. F4. Mudstone with minor sandstone, consisting primarily of B5 and minor B4 and may appear massive, laminated, or heterolithic. F5. Disturbed mudstone and sandstone, which consists of a single B6 deposit or multiple stacked B6 deposits separated by erosional surfaces or thin laminated mudstones. In addition to our dataset, F5 has been reported from the subsurface of the Lynn Mountain Syncline (Legg et al., 1990) and poorly exposed outcrops in the Ti Valley of Oklahoma (Suneson and Ferguson, 1987) (Table 1).

We used four types of facies associations to cover four broad groups of depositional environments of the lower Atoka (Fig. 6 & Table 4): FA1-Channel, FA2-Lobe, FA3-Mudstone sheet, and FA4-Mass transport deposit (MTD) (Prather et al., 2000; Slatt et al., 2000; Slatt and Stone, 2001; Nilsen et al., 2007; Pyles et al., 2008; Zou et al., 2012; Grundvåg et al., 2014; Moscardelli and Wood, 2015). The criteria focus primarily on the

bounding surfaces and lithofacies compositions and secondarily on geometric constraints (sensu Slatt et al., 2000; Zou et al., 2012). The definitions and characteristics are listed in Table 4, outcrop examples are given in Figure 6, and brief descriptions are as follows:

A channel (FA1) is defined by a > 0.5 m relief erosional surface at the base and by the beginning of a tabular sandstone or mudstone interval at the top (Figs. 6 & 7). Beds show rapid changes in thickness and dip within an outcrop. A channel may have multiple internal erosional surfaces or scours. The channel deposits in this study are equivalent to the ‘channel elements’ or ‘single-story channels’ in the Brushy Canyon Formation in Texas (Carr and Gardner, 2000; Gardner et al., 2003), the Ross Formation in Ireland (Pyles, 2007), the Morrilo 1 member in Spain (Moody et al., 2012), and the Frysjaodden Formation in Spitsbergen (Grundvåg et al., 2014).

A lobe (FA2) is defined by a tabular, non-erosive or locally erosive (< 0.5 m relief) surface at the base and the beginning of a mudstone interval (>0.4 m) at the top (Figs. 6 & 7). There is no visible change in bed thickness or dip within an outcrop. The sandstones are commonly structured and graded. The lobe deposits in this study are most equivalent to the ‘terminal splays’ of the Upper Kaza Group in British Columbia (Terlaky et al., 2016), the Ross Formation in Ireland (Pyles, 2007), the Frysjaodden Formation in Spitsbergen (Grundvåg et al., 2014), and the Skoorsteenbergs Formation in South Africa (Prélat et al., 2009).

A mudstone sheet (FA3) is defined by a minimum thickness threshold (0.4 m) and predominant F4 in lithofacies composition. The thickness threshold of 0.4 m was determined with reference to the thickness thresholds of ‘interlobe’ and ‘interlobe element’ in the Skoorsteenbergs Formation (Prélat et al., 2009) and the Frysjaodden Formation (Grundvåg et al., 2014).

A mass transport deposit (FA4) is the deposit of a single or multiple mass failure events that is not within a channel (FA1). FA4 may include thin mudstone intervals (<0.4 m) between separate events. Descriptions and interpretations of each composite section are given in Table 5 and examples of outcrop photo panels are shown in Figs. 8, 9, 12, and 14.

Longitudinal facies distribution in the foredeep

The longitudinal facies variation in the foredeep is characterized by 11 composite sections (Figs. 8 & 9, Tables 1 & 5). To simplify the correlation, the following three pairs of composite sections: S4-S5, S6-S7, S8-S9, with the same longitudinal locations are grouped. The paleoflow of S3-S11 is predominantly east to west, which concurs with previous depositional models (Figs. 3 & 4). The paleoflow at S4 trends northwest, possibly reflecting local flow deflections due to topographic obstacles.

In the western foredeep, S13 shows eastward and northeastward paleoflow directions (Fig. 10). This area reflects sediment supply from the west, likely the Arbuckle Mountains (Archinal, 1979; Ferguson and Suneson, 1988). The paleoflow directions at S12 show a unique bimodal pattern (Fig. 10), which reflects the co-existence of two opposing axial submarine fan systems (Ferguson and Suneson, 1988; Sharrah, 2006) and potentially complex basin floor topography in this area. S12 likely represents a mixing zone and the distal or lateral portions of both fan systems. For all localities, no discrepancy is found in the paleoflow between thicker-bedded sandstones (B1-B2) and thinner-bedded sandstones (B3-B4). The standard deviations of paleocurrents are overall low except for S12.

The longitudinal facies distributions of both thickness proportions and normalized frequencies of all hierarchical orders generally follow the mean paleoflow directions (Fig. 10). From S3 to S11 and from S13 to S11, there is an overall decrease in sandy facies and an increase in muddy facies (Fig. 10). There is also a gradual decrease from east to west in mass

transport deposits (Fig. 10). In the eastern foredeep, S6-S7 exhibit the highest values in thickness proportions of sandy facies, percent sandstone, and amalgamation ratio.

Asymmetrical facies distribution in the Fourche La Fave Syncline

The Fourche La Fave Syncline (FLFS) in Arkansas, which is ~20 km wide and over 120 km long, is the largest structure in the foredeep (Fig. 11, Tables 1 & 5). The FLFS is the main component of the foredeep and possibly active during the deposition of lower Atoka (Arbenz, 2008). The high density of outcrops in this study allows us to compare the facies distribution between the north (S4, S6, S8) and the south limbs (S5, S7, S9, S10) of the FLFS. Data shows a subtle difference between the north and south limbs of the FLFS in paleocurrent patterns, except for the S4 locality (Fig. 11). The standard deviation of paleocurrent directions is ~25 degrees. The paleoflow shows only subtle differences between thicker-bedded sandstones (B1-B2) and thinner-bedded sandstones (B3-B4). However, the facies compositions do show an important difference between the north and south. The thickness proportions of sandy facies components increase from east to west in the north limb but remain relatively constant in the south limb (Fig. 11). The normalized frequencies show a similar contrast between the north and south but to a lesser extent. Additionally, the contrast is more obvious in the amalgamation ratio profile than that in the percent sandstone profile.

Longitudinal facies distribution in wedge-top zone

The facies distribution in the wedge-top is characterized by five composite sections (Figs. 12 & 13, Tables 1 & 5). The eastern (S14-S15) and the western (S16-S18) sections represent the proximal and distal localities, respectively (Fig. 4), although the former ones are not necessarily the direct updip equivalents to the latter due to uncertain correlation. The mean paleoflow directions are due west and southwest, following the structural strike and basin axis but with some deviations (Fig. 13). At S14-S15, a small portion of northward paleocurrent directions is found in some thick-bedded sandstones. At S16, the paleoflow

exhibits a tri-modal pattern which is due northwest, southwest, and south (Fig. 13). The southwestward component of this pattern is found in thick-bedded sandstones. The standard deviations of the paleocurrent data are relatively high at S14-S16 and low at S17-S18.

The axial facies distribution of the wedge-top (Fig. 13) is counter-intuitive to conceptual submarine fan models (Bouma, 1962; Mutti and Ricci-Lucchi, 1978; Walker, 1978; Mutti, 1985; Bouma, 2000). The facies metrics are similar for S14 and S15 but more variable for S16-S18. From S14 to S16, the sandy facies decrease in both thickness proportions and normalized frequency, then increase rapidly from S16 to S18 (Fig. 13). In general, a classical proximal-distal facies trend is not well-defined in the wedge-top (Fig. 13B). Instead, the facies compositions are more stable (except S18), comparing to that in the foredeep.

Facies contrast in the continental foreland

Exposures along the southern margin of the continental foreland zone are limited. We selected two lower Atoka localities (S1 & S2) to show the contrast in depositional styles along the southern margin of the continental foreland (Figs. 14 & 15, Tables 1 & 5). The paleoflow in S1 exhibits a bi-modal pattern. The southward portion is found in thick-bedded channel-fill sandstones and the westward portion in isolated thin-bedded sandstones within thick laminated mudstone intervals. The paleocurrent directions at S2 are due east and show no discrepancy between the thicker- and thinner-bedded sandstones. Similar to S13 at the western end of the foredeep, S2 also reflects localized sediment input, likely from the Arbuckle region (Fig. 1B). Both localities are important in delineating the northern and western boundaries of sediment gravity flow deposition in the lower Atoka. Compared to the foredeep localities, S1 and S2 provide evidence of potential interactions between the smaller, marginal fans fed by local sources and the axial fan fed by the eastern source (Houseknecht, 1986; Ferguson and Suneson, 1988).

DISCUSSION

Potential limitations and advantages of the dataset

Although this study integrates the most extensive dataset that exists for lower Atoka outcrops, we recognize the limitations in this dataset and our associated interpretations and correlations. For instance, the total amount of data is small compared to the volume of the depositional system. In addition, sandstone intervals are preferentially exposed due to weathering. In Lynn Mountain Syncline in Oklahoma, the percent sandstones from the outcrops are typically 50-70% whereas subsurface data suggests <40% (Legg et al., 1990), suggesting that mudstone intervals are likely underrepresented by 10-30% in our dataset. Additionally, abundant channels and mass transport deposits are present in basal Atoka wedge-top locales (Walthall, 1967; Legg et al., 1990), which might also be underrepresented in our dataset. Most measured sections compiled from the literature are very detailed, but sometimes the outcrops were no longer accessible. In those cases, we had to reinterpret the sections into our framework with limited information. We also emphasize that we do not attempt to perform bed-scale correlations between sections, but instead focus on system-scale variability in lithology and facies compositions.

On the positive side, the outcrops of the lower Atoka occur semi-randomly in both spatial and temporal sense, which is preferred for statistical sampling. The total measured thickness in proximal and distal localities in the foredeep and wedge-top is proportional to the total thicknesses of Atoka deposits in these regions. This indicates the sample sizes are similar if normalized by the preserved deposit volume in the four regions.

Interpreting channels and lobes in the lower Atoka

While mudstone sheets and mass transport deposits are relatively easy to identify, interpreting channel and lobe architectures can be challenging on outcrops with limited lateral extents, like those of the lower Atoka. We acknowledge this difficulty and therefore compare our results to some well-exposed, well-documented deepwater outcrops. The channel deposits (FA1) account for 8.1% of the lower Atoka by thickness. The thickness range of channel deposits is 0.5-16 m and they are typically 1-8 m thick (Table 4), which is comparable to many other channel deposits in the study area and around the world. For example, the thickness ranges of single-channel deposits are approximately 11-23 m in the middle Atoka (Xu et al., 2009) and 2-23 m in the Jackfork Group (Olariu et al., 2011) for slope settings, and typically less than 15 m in the Jackfork for basinal settings (Brito et al., 2012; Zou et al., 2012, 2017). Globally, similar thickness ranges are documented from the ‘single story channels’ in the Brushy Canyon Formation in Texas, the ‘channel (element)’ in the Ross Formation in Ireland (Pyles, 2007), the ‘channel element’ in the Morrilo 1 member of Ainsa Basin in Spain (Moody et al., 2012), and the ‘channel element’ in the Frysjaodden Formation in Spitsbergen (Grundvåg et al., 2014). We also acknowledge the wide range of channel dimensions from other ancient and modern examples depending on the definitions and the nature of the depositional systems (Clark and Pickering, 1996; Jobe et al., 2016; Cullis et al., 2018; Pettinga et al., 2018; Shumaker et al., 2018).

Similar to channel deposits, there is also a wide range of dimensions and definitions of lobe deposits (Deptuck et al., 2008; Cullis et al., 2018; Pettinga et al., 2018), which we attempt to reconcile with our dataset. Lobe deposits (FA2) account for 51% of the lower Atoka dataset by thickness. The thickness range is 0.26-21 m and they are typically 0.5-6 m in thickness (Table 4). In the study area, this thickness range is comparable to the ‘sheet’ element in the Jackfork Group (Slatt et al., 2000; Zou et al., 2012, 2017). The range of lobe thickness in our dataset is comparable globally to the ‘terminal splay’ of the Upper Kaza

Group in British Columbia (Terlaky et al., 2016), the ‘lobe (element)’ of the Ross Formation in Ireland (Pyles, 2007), the ‘lobe element’ and ‘lobe’ of the Frysjaodden Formation in Spitsbergen (Grundvåg et al., 2014), and the ‘lobe element’ and ‘lobe’ of the Skoorsteenbergt Formation in Tanqua-Karoo Basin (Prélat et al., 2009). The lobe deposits with thicknesses < 1 m in the lower Atoka are primarily isolated tabular sandstone packages within thick mudstone intervals. Instead of lumping them into mudstone sheet (FA3), we interpret them as distal lobe or lobe fringe deposits (Prélat et al., 2009; Terlaky et al., 2016; Sychala et al., 2017).

Major controls on the stratigraphic patterns in the foredeep and foreland

The spatial variations of the facies distribution in the foredeep appear to be primarily controlled by the interplay of sediment supply and basin configuration. The development of the OFTB migrated from east to west during Carboniferous (Thomas, 2004; Arbenz, 2008; Johnson, 2011). As a result, the subsidence and accommodation in the eastern foredeep are at least twice as much as that in the west (Arbenz, 2008; Johnson, 2011). The paleo Y City Fault on the south and the continental shelf-slope on the north probably provided structural confinement for the foredeep. The evidence of syn-depositional structural movement includes (A) basin-wide rapid subsidence of basal Atoka shelf deposits (known as the Spiro Sandstone) in the continental foreland (Houseknecht, 1986; Saleh, 2004; Denham, 2018), (B) stratigraphic onlap onto emerging anticlinal structures in southwestern foreland (Archinal, 1979), and (C) fault-induced basin compartmentalization in the western foredeep (Ferguson and Suneson, 1988; Dickinson et al., 2003; Sharrah, 2006). The patterns of paleoflow and facies distribution show that the foredeep received sediments from the east, north, and west (Fig. 10). The eastern source provided most of the sediments, as supported by regional studies on sandstone petrography (Graham et al., 1976; Sprague, 1985), detrital zircon geochronology (Sharrah, 2006), and isotope geochemistry (Gleason et al., 1995). The

influence of the eastern source is much diminished in the western quarter of the foredeep (Fig. 10). We can deduce that the sediment supply from the Laurentian craton to the north was probably trivial comparing to that from the east. Although slope channel systems have been recognized in the middle Atoka (Houseknecht and McGilvery, 1990; Xu et al., 2009), they might not have been well-developed in the lower Atoka (*sensu* Saleh, 2004; Denham, 2018). The presence of the western source is supported by facies distribution, paleocurrent analysis (Ferguson and Suneson, 1988; Sharrah, 2006), sandstone petrography ('Arbuckle facies', Houseknecht, 1986), structural history and paleogeography (Sutherland, 1982; Golonka et al., 2007), but its influence may also have been limited and localized.

The asymmetrical facies distribution in Fourche La Fave Syncline (FLFS) in the eastern foredeep is supported by qualitative observations (Table 1) and previous investigations (Fulton, 1985; LaGrange, 2002), but the reason for its occurrence is not well understood. The structural history suggests that deposition was coeval with the development of the Y City Fault and the syncline (Arbenz, 2008; Johnson, 2011). The pre-folded width of the syncline is less than 30 km. We compared three candidate interpretations for the asymmetrical facies distribution: (A) axial vs marginal locations inferred from classical and modern fan models (Walker, 1978; Mutti, 1985; Mutti and Normark, 1987; Pr elat et al., 2009), (B) influence of additional sediment supply from the northern margin, and (C) influence of thrust-related topographic confinement to the south. For unconfined fans, compensational stacking (Straub et al., 2009) would distribute deposit thickness evenly over time, and nearby sections are expected to show similar facies compositions at the system scale (Marini et al., 2015; Liu et al., 2018). Therefore, such classical model-based interpretation (interpretation 'A' above) cannot explain the facies asymmetry in the FLFS. Interpretation 'B' depends on the assumption that the local source must preferentially feed the northern side of the later FLFS but not 20-30 km further south. This interpretation is

unrealistic without other mechanisms to constrain sediments to the northern side of the syncline. Therefore, we favor interpretation ‘C’ because (1) asymmetrical facies distributions and rapid facies change within short distances are characteristic in laterally confined settings (Cunha et al., 2017; Tinterri et al., 2017; Pinter et al., 2018), (2) the Y City Fault was already active and would conveniently induce seafloor tilting and provide some degree of topographic confinement, and (3) no additional assumptions are needed to arrive at this solution.

Major controls on the stratigraphic patterns in the wedge-top

The facies distribution in the wedge-top is controlled by the interplay of sediment supply and structural development. The sediment transport is primarily axial in the wedge-top. The sediments in southeastern wedge-top (i.e. Athens Plateau) were thought to be derived from the east and southeast (Walthall, 1967; Gleason et al., 1994; Thomas, 1997; Thomas et al., 2019). The southeastern wedge-top is overall similar to the eastern foredeep in facies composition, amalgamation ratio (Figs. 10 & 13), and sandstone petrography (Graham et al., 1976; Sprague, 1985). However, it differs from the eastern foredeep by overall greater sandstone proportions, more abundant plant fragments, and lack of trace fossils. Previous studies also suggest that the southeastern wedge-top has horizons of mold fauna at the base of turbidite sandstones (Walthall, 1967; Sprague, 1985), which may indicate shallower water depth or proximity to shallow-marine settings.

The most important feature of the wedge-top is the persistence of the dynamic facies characteristics in both proximal and distal locations, which may result from (A) additional sediment sources along the southern margin of the basin or (B) structural confinement. The southern extent of the basin margin is poorly understood, and there is a lack of direct evidence of sediment supplies from the peri-Gondwana terranes. Isotope geochemistry (Gleason et al., 1995) and sandstone petrography (Banjade and Kerr, 2015) suggest recycled

orogen of Appalachian affinity for these deposits, although these signatures might be difficult to distinguish from proto-Ouachita highlands (Thomas, 2004). This suggests that the eastern source is dominant in the wedge-top and the influence from other sources is likely to be minor.

The role of structural control on deposition in the wedge-top has not been widely discussed in the study area. The inherited topography (*sensu* Sømme et al., 2019) on wedge-top basins and associated syn-depositional structural movements (*sensu* Felletti, 2002; Tinterri and Tagliaferri, 2015) can modify the degree of lateral confinement and the local gradient of the basin floor, both of which can have a significant influence on depositional styles (*sensu* Mccaffrey and Kneller, 2004; Wynn et al., 2012). The central uplift in the Ouachita wedge-top, the Benton and Broken Bow uplifts (BU-BBU)(Nelson et al., 1982; Arbenz, 2008; Johnson, 2011), may have an important influence on the deposition. The BU is the uppermost part of the Ouachita accretionary wedge (Thomas, 2004). The duration of the basement uplift of the BU is dated as 339 ± 19 to 307 ± 39 Ma (Johnson, 2011), which probably encompassed the entire Stanley-Atoka succession. The development of the central uplift was likely episodic, although the uplifts were not necessarily subaerial. Evidence for this episodic uplift includes (A) the conglomerates-breccias in the Hot Spring Sandstone (Lower Stanley Group, Morris, 1974; Niem, 1976; Godo et al., 2014), (B) the contrast in the amount of disturbed facies in the Jackfork Group north and south of BU (Morris, 1974a), (C) the wedge-top wide distribution of olistostromes in the Johns Valley Formation (Walthall, 1967; Shideler, 1970; Dickinson et al., 2003), and (D) the wedge-top wide distribution of channel incisions, mass transport deposits (including olistostromes) stratigraphically near the basal Atoka (Walthall, 1967; Legg et al., 1990). Due to its size and magnitude, the BU-BBU could have served as an elongate intra-basinal high and facilitated axial sediment transport during

the deposition of the lower Atoka and resulted in the persistent dynamic facies characteristics (Fig. 16).

Comparison to other structurally complex basins

The lower Atoka formation represents the basin fill during the early phase of terrane-continent collision and accretionary prism growth, a structurally analogous setup to coeval foreland basin deepwater deposits in the Marathon region in west Texas (Wuellner et al., 1986) as well as the Eocene-Early Miocene development of the Carpathian foreland basin (Golonka et al., 2007). The lower Atoka deepwater system is predominantly axially-sourced, typical for underfilled, deep marine foreland basins (Hubbard et al., 2008; Sharman et al., 2018). Contrasting depositional styles between the foredeep and the wedge-top, as seen in the lower Atoka (Fig. 16), have been widely documented in deepwater foreland basins (Mutti et al., 2003; Ricci-Lucchi, 2003; DeCelles, 2012), including the Alpine (Lomas and Joseph, 2004), Apennine (Ricci-Lucchi, 1986; Covault et al., 2009), and Magallanes foreland basins (Bernhardt et al., 2011). Intrabasinal structures may exert a fundamental control on stratigraphic architecture, and the asymmetrical facies distribution we document in the Fourche La Fave Syncline is comparable to that of the Firenzuola (Marnoso-Arenacea) turbidite system (Tagliaferri and Tinterri, 2016) and the Ranzano Sandstone (Tinterri et al., 2017) in the northern Apennines, and the Annot Sandstone in Peira Cava Basin (Cunha et al., 2017) In particular, wedge-top locales tend to exhibit syn-depositional deformation that affects stratigraphic architecture (Covault et al., 2009; Sinclair, 2012), and the lower Atoka in the wedge-top is laterally confined due to inherited and syn-depositional deformation (Fig. 16). This partial confinement is quite analogous to the Annot Sandstone in southeastern France (Salles et al., 2014), the Miocene wedge-top depozone of Sicilian foreland (Covault et al., 2009; Pinter et al., 2016), the piggyback basins in the Pyrenees (Puigdefàbregas et al.,

1986; Remacha et al., 2003; Sutcliffe and Pickering, 2009), the Neogene trench-slope basins in New Zealand (Burgreen and Graham, 2014). Our study provides statistics on the bed, facies, and element thicknesses that can aid in recognition (Marini et al., 2015) and interpretation of these settings.

CONCLUSIONS

This study quantitatively documents the facies compositions of the lower Atoka deepwater system in three structural-depositional zones of the Greater Arkoma Basin: foredeep, wedge-top, and southern foreland. The foredeep is characterized by two axial fan systems: the main west-prograding fan and the small east-prograding fan near the western margin. The sand-rich facies components decrease rapidly along the sediment transport pathways for both fan systems. The asymmetrical facies distribution in the Fourche La Fave Syncline in the eastern foredeep suggests potential lateral confinement induced by thrust-related tilting. The wedge-top is characterized by relatively stable facies compositions along the sediment transport pathway, most likely due to strong lateral confinement provided by intra-basinal highs. The foreland outcrops suggest the presence of a slope-channel system on the northern margin and small east-prograding fan system on the western basin-margin, although their contribution may have been volumetrically limited. We interpret that the depositional styles in the three zones are due to different combinations of structural framework, syn-depositional tectonics, sediment supply, and paleogeographic configuration. This study provides an updated and relatively complete understanding of the lower Atoka deepwater system. The methods and results have implications for analogous depositional systems along the Appalachian-Ouachita fold and thrust belt, as well as in global rift basins and fold and thrust belt basins.

ACKNOWLEDGMENTS

This study is part of the PH's doctoral research funded by the Chevron Center of Research Excellence (CoRE, <https://core.mines.edu/>) and the Sedimentary Analogs Database research program (SAnD, <https://geology.mines.edu/research/sand/>) at the Colorado School of Mines. We thank Hang Deng and Jingqi Xu for field assistance, Cathy Van Tassel and Debora Cockburn for logistical support, Dough Hanson (Arkansas Geological Survey) for local geology, local landowners for outcrop access in quarries, and Nick Howes and John Martin for technical support with MATLAB.

REFERENCES

- AL-SIYABI, H.A., 2000, Anatomy of a Type II Turbidite Depositional System: Upper Jackfork Group, DeGray Lake Area, Arkansas, in Bouma, A.H. and Stone, C.G., eds., *Fine-Grained Turbidite Systems*, AAPG Memoir 72 / SEPM Special Publication 68: American Association of Petroleum Geologists, Tulsa, Oklahoma, p. 245–261.
- AL-SIYABI, H.A., 1998, Sedimentology and stratigraphy of the early Pennsylvanian Upper Jackfork interval in the Caddo Valley quadrangle, Clark and Hot Spring counties, Arkansas: Colorado School of Mines, 272 p.
- ALLEN, P.A., and ALLEN, J.R., 2005, *Basin analysis: Principles and applications*: Blackwell Publishing Ltd, Malden, MA, USA; Oxford, OX, UK; Carlton, Australia, 549 p.
- ARBENZ, J.K., 1989, Ouachita thrust belt and Arkoma Basin, in Hatcher, R.D., Thomas, W.A., and Viele, G.W., eds., *The Appalachian-Ouachita Orogen in the United States*: Geological Society of America, Norman, Oklahoma, Oklahoma, p. 621–634.
- ARBENZ, J.K., 2008, Structural framework of the Ouachita Mountains, in Suneson, N.H., ed., *Stratigraphic and Structural Evolution of the Ouachita Mountains and Arkoma Basin, Southeastern Oklahoma and West-Central Arkansas: Applications to Petroleum Exploration 2004 Field Symposium (The Arbenz-Misch/Oles Volume)*: Oklahoma Geological Survey, Norman, Oklahoma, p. 1–42.
- ARCHINAL, B.E., 1979, Atoka Formation (Pennsylvanian) Deposition and Contemporaneous Structural Movement, Southwestern Arkoma Basin, Oklahoma (N. J. Hyne, Ed.): Tulsa Geological Society, Tulsa, Oklahoma, 259–267 p.
- ARNE, D.C., 1992, Evidence from Apatite Fission-Track Analysis for Regional Cretaceous Cooling in the Ouachita Mountain Fold Belt and Arkoma Basin of Arkansas: *American Association of Petroleum Geologists Bulletin*, v. 76, p. 392–402.
- BABAEI, A., and VIELE, G.W., 1992, Two-decked nature of the Ouachita Mountains, Arkansas: *Geology*, v. 20, p. 995–998, doi: 10.1130/0091-7613(1992)020<0995:TDNOTO>2.3.CO;2.
- BANJADE, B., and KERR, D., 2015, Tectonostratigraphic evolution of the Ouachita trough through the study of the deepwater Atoka sandstone and mudrock from central Ouachita, SE Oklahoma: Implication for Rheic Ocean closure (Abstract): *American Association of Petroleum Geologists Search and Discovery*, v. 90221.
- BERNHARDT, A., JOBE, Z.R., and LOWE, D.R., 2011, Stratigraphic evolution of a submarine channel-lobe complex system in a narrow fairway within the Magallanes foreland basin, Cerro Toro Formation, southern Chile: *Marine and Petroleum Geology*, v. 28, p. 785–806, doi: 10.1016/j.marpetgeo.2010.05.013.

- BOUMA, A.H., 2000, Fine-grained, mud-rich turbidite systems: model and comparison with coarse-grained, sand-rich systems, in Bouma, A.H. and Stone, C.G., eds., *Fine-Grained Turbidite Systems*, AAPG Memoir 72 / SEPM Special Publication 68: American Association of Petroleum Geologists & SEPM(Society for Sedimentary Geology), Tulsa, Oklahoma, p. 9–20.
- BOUMA, A.H., 1962, *Sedimentology of some Flysch deposits: a graphic approach to facies interpretation*: Elsevier Pub. Co., Amsterdam; New York, 168 p.
- BRIGGS, G., 1974, Carboniferous Depositional Environments in the Ouachita Mountains-Arkoma Basin Area of Southeastern Oklahoma: Geological Society of America Special Paper, v. 148, p. 225–239, doi: 10.1130/SPE148-p225.
- BRITO, R.J., CASTILLO, L.A., OSWALDO, D., CADENA, A., and SLATT, R.M., 2012, Multidisciplinary Data Integration for 3D Geological Outcrop Characterization - Jackfork Group, Hollywood Quarry Arkansas, in AAPG Search and Discovery.:
- BURGREEN, B., and GRAHAM, S.A., 2014, Evolution of a deep-water lobe system in the Neogene trench-slope setting of the East Coast Basin, New Zealand: Lobe stratigraphy and architecture in a weakly confined basin configuration: *Marine and Petroleum Geology*, v. 54, p. 1–22, doi: 10.1016/j.marpetgeo.2014.02.011.
- CARR, M., and GARDNER, M.H., 2000, Portrait of a Basin-Floor Fan for Sandy Deep-Water Systems, Permian Lower Brushy Canyon Formation, West Texas, in Bouma, A.H. and Stone, C.G., eds., *Fine-Grained Turbidite Systems*, AAPG Memoir 72 / SEPM Special Publication 68: American Association of Petroleum Geologists & SEPM (Society for Sedimentary Geology), Tulsa, Oklahoma, p. 215–231.
- CHAMBERLAIN, C.K., 1971, Bathymetry and Paleoecology of Ouachita Geosyncline of Southeastern Oklahoma as Determined from Trace Fossils: *American Association of Petroleum Geologists Bulletin*, v. 55, p. 34–50, doi: 10.1306/5D25CDD3-16C1-11D7-8645000102C1865D.
- CLARK, C.J., BOUMA, A.H., and CONSTANTINE, G.A., 1999, Turbidites from the Lower Atoka Formation, Jacksonville, Arkansas: *Gulf Coast Association of Geological Societies Transactions*, v. 49, p. 172–182.
- CLARK, C.J., BOUMA, A.H., and SAMUEL, B.M., 2000, Shale morphology and seal characterization of the Lower Atoka Formation deepwater deposits, Jacksonville, Arkansas: *Gulf Coast Association of Geological Societies Transactions*, v. 50, p. 591–606.
- CLARK, J.D., and PICKERING, K.T., 1996, Architectural Elements and Growth Patterns of Submarine Channels: Application to Hydrocarbon Exploration: *American Association of Petroleum Geologists Bulletin*, v. 80, p. 194–221.
- CLINE, L.M. (ed.), 1968, *A guidebook to the geology of the western Arkoma Basin and Ouachita Mountains*, Oklahoma: Oklahoma City Geological Society, Oklahoma City, 62 p.

- COLEMAN, J.L., 2000, Carboniferous submarine basin development of the Ouachita Mountains of Arkansas and Oklahoma, in Bouma, A.H. and Stone, C.G., eds., AAPG Memoir 72 / SEPM Special Publication No. 68: Fine-Grained Turbidite Systems: The American Association of Petroleum Geologists and SEPM (Society for Sedimentary Geology), p. 21–32.
- COVAULT, J.A., HUBBARD, S.M., GRAHAM, S.A., HINSCH, R., and LINZER, H.G., 2009, Turbidite-reservoir architecture in complex foredeep-margin and wedge-top depocenters, Tertiary Molasse foreland basin system, Austria: *Marine and Petroleum Geology*, v. 26, p. 379–396, doi: 10.1016/j.marpetgeo.2008.03.002.
- CULLIS, S., COLOMBERA, L., PATACCI, M., and MCCAFFREY, W.D., 2018, Hierarchical classifications of the sedimentary architecture of deep-marine depositional systems: *Earth-Science Reviews*, v. 179, p. 38–71, doi: 10.1016/j.earscirev.2018.01.016.
- CUNHA, R.S., TINTERRI, R., and MAGALHAES, P.M., 2017, Annot Sandstone in the Peira Cava basin: An example of an asymmetric facies distribution in a confined turbidite system (SE France): *Marine and Petroleum Geology*, v. 87, p. 60–79, doi: 10.1016/j.marpetgeo.2017.04.013.
- DAVYDOV, V.I., CROWLEY, J.L., SCHMITZ, M.D., and POLETAEV, V.I., 2010, High-precision U-Pb zircon age calibration of the global Carboniferous time scale and Milankovitch band cyclicity in the Donets Basin, eastern Ukraine: *Geochemistry, Geophysics, Geosystems*, v. 11, p. 1–22, doi: 10.1029/2009GC002736.
- DECELLES, P.G., 2012, Foreland Basin Systems Revisited: Variations in Response to Tectonic Settings, in Busby, C. and Azor, A., eds., *Tectonics of Sedimentary Basins*: John Wiley & Sons, Ltd, Chichester, UK, p. 405–426.
<https://doi.org/10.1002/9781444347166.ch20>.
- DENHAM, W.S., 2018, Subsurface stratigraphic interpretation of the Lower Atoka Formation, Northern Arkoma Basin, Arkansas: University of Arkansas, Fayetteville, 92 p.
- DEPTUCK, M.E., PIPER, D.J.W., SAVOYE, B., and GERVAIS, A., 2008, Dimensions and architecture of late Pleistocene submarine lobes off the northern margin of East Corsica: *Sedimentology*, v. 55, p. 869–898, doi: 10.1111/j.1365-3091.2007.00926.x.
- DICKINSON, W.R., PATCHETT, P.J., FERGUSON, C.A., SUNESON, N.H., and GLEASON, J.D., 2003, Nd isotopes of Atoka Formation (Pennsylvanian) turbidites displaying anomalous east-flowing paleocurrents in the frontal Ouachita belt of Oklahoma: Implications for regional sediment dispersal: *The Journal of Geology*, v. 111, p. 733–740.
- FELLETTI, F., 2002, Complex bedding geometries and facies associations of the turbiditic fill of a confined basin in a transpressive setting (Castagnola Fm, Tertiary Piedmont

- Basin, NW Italy): *Sedimentology*, v. 49, p. 645–667, doi: 10.1046/j.1365-3091.2002.00467.x.
- FERGUSON, C.A., and SUNESON, N.H., 1988, Tectonic implications of Early Pennsylvanian paleocurrents from flysch in the Ouachita Mountains frontal belt, southeast Oklahoma, in Johnson, K.S., ed., *Shelf-to-Basin Geology and Resources of Pennsylvanian Strata in the Arkoma Basin and Frontal Ouachita Mountains of Oklahoma*. Oklahoma Geological Survey Guidebook 25: Oklahoma Geological Survey, Norman, Oklahoma, p. 49–61.
- FRYER, R.C., and JOBE, Z.R., 2019, Quantification of the bed-scale architecture of submarine depositional environments: *The Depositional Record*, v. 5, p. 192–211, doi: 10.1002/dep2.70.
- FULTON, D.A., 1985, *Sedimentology, structure, and thermal maturity of the lower Atoka formation, Ouachita frontal thrust belt, Yell and Perry counties, Arkansas*: University of Missouri, Columbia, 222 p.
- GARDNER, M.H., BORER, J.M., MELICK, J.J., MAVILLA, N., DECHESNE, M., and WAGERLE, R.N., 2003, Stratigraphic process-response model for submarine channels and related features from studies of Permian Brushy Canyon outcrops, West Texas: *Marine and Petroleum Geology*, v. 20, p. 757–787, doi: 10.1016/j.marpetgeo.2003.07.004.
- GAWTHORPE, R.L., and LEEDER, M.R., 2000, Tectono-sedimentary evolution of active extensional basins: *Basin Research*, v. 12, p. 195–218, doi: 10.1111/j.1365-2117.2000.00121.x.
- GLEASON, J.D., 1994, Paleozoic tectonics and sediment sources of the Ouachita fold belt, Arkansas-Oklahoma and West Texas: an isotopic and trace element geochemical study: University of Arizona, 235 p.
- GLEASON, J.D., PATCHETT, P.J., DICKINSON, W.R., and RUIZ, J., 1994, Nd isotopes link Ouachita turbidites to Appalachian sources: *Geology*, v. 22, p. 347–350, doi: 10.1130/0091-7613(1994)022<0347:NILOTT>2.3.CO;2.
- GLEASON, J.D., PATCHETT, P.J., RUIZ, J., DICKINSON, W.R., and RUIZ, J., 1995, Nd isotopic constraints on sediment sources of the Ouachita-Marathon fold belt: *Geological Society of America Bulletin*, v. 107, p. 1192–1210.
- GODO, T., LI, P., and RATCHFORD, M.E., 2014, A Geological Overview of the Shell Arivett No.1-26 Well, Pike County, Arkansas: *Shale Shaker*, v. 65, p. 34–64.
- GOLONKA, J., SLACZKA, A., and PICHA, F.J., 2007, The West Carpathians and Ouachitas: A comparative study of geodynamic evolution, in Golonka, J. and Picha, F.J., eds., *The Carpathians and Their Foreland: Geology and Hydrocarbon Resources*. AAPG Memoir 84: American Association of Petroleum Geologists, Tulsa, Oklahoma, p. 787–810.

- GRAHAM, S.A., DICKINSON, W.R., and INGERSOLL, R. V., 1975, Himalayan-Bengal Model for Flysch Dispersal in the Appalachian-Ouachita System: *Geological Society of America Bulletin*, v. 86, p. 273, doi: 10.1130/0016-7606(1975)86<273:HMFFDI>2.0.CO;2.
- GRAHAM, S.A., INGERSOLL, R. V., and DICKINSON, W.R., 1976, Common provenance for lithic grains in Carboniferous sandstones from Ouachita Mountains and Black Warrior Basin: *Journal of Sedimentary Petrology*, v. 46, p. 1–8.
- GRUNDVÅG, S., JOHANNESSEN, E.P., HELLAND-HANSEN, W., and PLINK-BJÖRKLUND, P., 2014, Depositional architecture and evolution of progradationally stacked lobe complexes in the Eocene Central Basin of Spitsbergen: *Sedimentology*, v. 61, p. 535–569, doi: 10.1111/sed.12067.
- HALEY, B.R., GLICK, E.E., BUSH, W. V., CLARDY, B.F., STONE, C.G., WOODWARD, M.B., and ZACHRY, D.L., 1993, *Geologic Map of Arkansas*. Scale 1:500 000 (N. F. Williams & D. A. Peck, Eds.): U.S. Geological Survey & Arkansas Geological Commission, Little Rock, Arkansas, 1 p.
- HALEY, B.R., and STONE, C.G., 1994, *Explanation for the geologic maps of the Ouachita Mountains and southern Arkoma Basin, Arkansas*. Scale 1: 100 000: Arkansas Geological Commission, Little Rock, 50 p.
- HALEY, B.R., and STONE, C.G., 2006, *Geologic Map of the Ouachita Mountain Region and a Portion of the Arkansas River Valley Region in Arkansas* 1:125 000 (W. D. Hanson, Ed.): Arkansas Geological Commission, Little Rock, Arkansas, 1 p.
- HANSEN, L.A.S., CALLOW, R., KANE, I., and KNELLER, B., 2017, Differentiating submarine channel-related thin-bedded turbidite facies: Outcrop examples from the Rosario Formation, Mexico: *Sedimentary Geology*, v. 358, p. 19–34, doi: <https://doi.org/10.1016/j.sedgeo.2017.06.009>.
- HARRY, D.L., and MICKUS, K.L., 1998, Gravity constraints on lithosphere flexure and the structure of the late Paleozoic Ouachita orogen in Arkansas and Oklahoma, south central North America: *Tectonics*, v. 17, p. 187–202, doi: 10.1029/97tc03786.
- HATCHER, R.D., THOMAS, W.A., and VIELE, G.W., 1989, *The Appalachian-Ouachita Orogen in the United States*. Vol F-2 (R. D. Hatcher, W. A. Thomas, & G. W. Viele, Eds.): Geological Society of America, Boulder, Colorado, 782 p. <https://pubs.geoscienceworld.org/books/book/862/>.
- HAUGHTON, P.D.W., BARKER, S.P., and MCCAFFREY, W.D., 2003, “Linked” debrites in sand-rich turbidite systems - Origin and significance: *Sedimentology*, v. 50, p. 459–482, doi: 10.1046/j.1365-3091.2003.00560.x.
- HAUGHTON, P.D.W., DAVIS, C., MCCAFFREY, W.D., and BARKER, S.P., 2009, Hybrid sediment gravity flow deposits - Classification, origin and significance: *Marine and Petroleum Geology*, v. 26, p. 1900–1918, doi: 10.1016/j.marpetgeo.2009.02.012.

- HECKEL, P.H., and CLAYTON, G., 2006, The Carboniferous System. Use of the new official names for the subsystems, series and stages: *Geologica Acta*, v. 4, p. 403–407, doi: 10.1016/S0016-7878(06)80045-3.
- HESSLER, A.M., and FILDANI, A., 2019, Deep-sea fans: tapping into Earth's changing landscapes: *Journal of Sedimentary Research*, v. 89, p. 1171–1179, doi: 10.2110/jsr.2019.64.
- HOUSEKNECHT, D.W., 1986, Evolution from passive margin to foreland basin: the Atoka Formation of the Arkoma Basin, south-central U.S.A., in Allen, P.A. and Homewood, P., eds., *Foreland Basins. Special Publication of International Association of Sedimentologists.*: Blackwell Publishing Ltd, Oxford, UK, p. 327–345.
- HOUSEKNECHT, D.W., COLEMAN, J.L., MILICI, R.C., GARRITY, C.P., ROUSE, W.A., FULK, B.R., PAXTON, S.T., ABBOTT, M.M., MARS, J.C., COOK, T.A., SCHENK, C.J., CHARPENTIER, R.R., KLETT, T.R., POLLASTRO, R.M., et al., 2010, Assessment of undiscovered natural gas resources of the Arkoma Basin Province and geologically related areas: U.S. Geological Survey Fact Sheet 2010-3043, p. 1–4, doi: 10.3133/fs20103043.
- HOUSEKNECHT, D.W., and MCGILVERY, T.A. (Mac), 1990, Red Oak Field, in *Structural Traps II: Traps Associated with Tectonic Faulting*: p. 201–225. <http://search.datapages.com/data/specpubs/fieldst3/data/a016/a016/0001/0200/0201.htm>.
- HUBBARD, S.M., ROMANS, B.W., and GRAHAM, S.A., 2008, Deep-water foreland basin deposits of the Cerro Toro Formation, Magallanes Basin, Chile: architectural elements of a sinuous basin axial channel belt: *Sedimentology*, v. 55, p. 1333–1359, doi: 10.1111/j.1365-3091.2007.00948.x.
- JOBE, Z.R., HOWES, N.C., and AUCHTER, N.C., 2016, Comparing submarine and fluvial channel kinematics: Implications for stratigraphic architecture: *Geology*, v. 44, p. 931–934, doi: 10.1130/G38158.1.
- JOBE, Z.R., SYLVESTER, Z., PARKER, A.O., HOWES, N., SLOWEY, N., and PIRMEZ, C., 2015, Rapid Adjustment of Submarine Channel Architecture to Changes in Sediment Supply: *Journal of Sedimentary Research*, v. 85, p. 729–753, doi: 10.2110/jsr.2015.30.
- JOHNSON, H.E., 2011, 3D structural analysis of the Benton Uplift, Ouachita Orogen, Arkansas: Texas A&M University, 238 p.
- KELLER, G.R., and HATCHER, R.D., 1999, Some comparisons of the structure and evolution of the southern Appalachian–Ouachita orogen and portions of the Trans-European Suture Zone region: *Tectonophysics*, v. 314, p. 43–68, doi: 10.1016/S0040-1951(99)00236-X.
- LAGRANGE, K.R., 2002, Characterization of the Lower Atoka Formation Arkoma Basin, Central Arkansas: Louisiana State University, 213 p.

- LEGG, T.E., LEANDER, M.H., and KRANCER, A.E., 1990, Exploration cast study: Atoka and Jackfork section, Lynn Mountain Syncline, Le Flore and Pushmataha counties, Oklahoma, in Suneson, N.H., Campbell, J.A., and Tilford, M.J., eds., *Geology and Resources of the Eastern Ouachita Mountains Frontal Belt and Southeastern Arkoma Basin, Oklahoma*. Oklahoma Geological Survey Guidebook 29: Oklahoma Geological Survey, Norman, Oklahoma, Oklahoma, p. 131–144.
- LILLIE, R.J., NELSON, K.D., VOOGD, B. de, BREWER, J.A., OLIVER, J.E., BROWN, L.D., KAUFMAN, S., and VIELE, G.W., 1983, Crustal Structure of Ouachita Mountains, Arkansas: A Model Based on Integration of COCORP Reflection Profiles and Regional Geophysical Data: *American Association of Petroleum Geologists Bulletin*, v. 67, p. 907–931, doi: 10.1306/03B5B6CD-16D1-11D7-8645000102C1865D.
- LIU, Q., KNELLER, B.C., FALLGATTER, C., BUSO, V.V., and MILANA, J.P., 2018, Tabularity of individual turbidite beds controlled by flow efficiency and degree of confinement: *Sedimentology*, v. 65, p. 2368–2387, doi: 10.1111/sed.12470.
- LOMAS, S.A., and JOSEPH, P., 2004, Confined turbidite systems, in Lomas, S.A. and Joseph, P., eds., *Confined Turbidite Systems*. Geological Society, London, Special Publications: The Geological Society of London, London, p. 1–7.
- MARINI, M., MILLI, S., RAVNÅS, R., and MOSCATELLI, M., 2015, A comparative study of confined vs. semi-confined turbidite lobes from the Lower Messinian Laga Basin (Central Apennines, Italy): Implications for assessment of reservoir architecture: *Marine and Petroleum Geology*, v. 63, p. 142–165, doi: 10.1016/j.marpetgeo.2015.02.015.
- MCCAFFREY, W.D., and KNELLER, B.C., 2004, Scale effects of non-uniformity on deposition from turbidity currents with reference to the Grès d'Annot of SE France, in Joseph, P. and Lomas, S.A., eds., *Deep-Water Sedimentation in the Alpine Basin of SE France: New Perspectives on the Grès Annot and Related Systems*: Geological Society, London, London, p. 301–310.
- MICKUS, K.L., and KELLER, G.R., 1992, Lithospheric Structure of the South-Central United-States: *Geology*, v. 20, p. 335–338, doi: 10.1130/0091-7613(1992)020<0335:lsotsc>2.3.co;2.
- MIDDLETON, G. V., and HAMPTON, M.A., 1973, Sediment gravity flows: mechanics of flow and deposition. S.E.P.M. Pacific Section Short Course Notes. Part I, in Middleton, G. V. and Bouma, A.H., eds., *Turbidites and Deep Water Sedimentation: SEPM*, Anaheim, California, p. 1–38.
- MOODY, J.D., PYLES, D.R., CLARK, J., and BOUROULLEC, R., 2012, Quantitative outcrop characterization of an analog to weakly confined submarine channel systems: Morillo 1 member, Ainsa Basin, Spain: *American Association of Petroleum Geologists Bulletin*, v. 96, p. 1813–1841, doi: 10.1306/01061211072.

- MORLEY, C.K., KING, R., HILLIS, R., TINGAY, M., and BACKE, G., 2011, Deepwater fold and thrust belt classification, tectonics, structure and hydrocarbon prospectivity: A review: *Earth-Science Reviews*, v. 104, p. 41–91, doi: 10.1016/j.earscirev.2010.09.010.
- MORRIS, R.C., 1974a, Carboniferous rocks of the Ouachita Mountains, Arkansas: A study of facies patterns along the unstable slope and axis of a flysch trough: *Geological Society of America Bulletin*, v. 148, p. 241–280, doi: 10.1130/SPE148-p241.
- MORRIS, R.C., 1971a, Classification and interpretation of disturbed bedding types in Jackfork flysch rocks (Upper Mississippian), Ouachita Mountains, Arkansas: *Journal of Sedimentary Petrology*, v. 41, p. 410–424, doi: - .
- MORRIS, R.C., 1974b, Sedimentary and tectonic history of the Ouachita Mountains, in Dickinson, W.R., ed., *Tectonics and Sedimentation*. SEPM Special Publication: SEPM (Society for Sedimentary Geology), p. 120–142.
- MORRIS, R.C., 1971b, Stratigraphy and sedimentology of Jackfork Group, Arkansas: *American Association of Petroleum Geologists Bulletin*, v. 55, p. 387–402, doi: 10.1306/5D25CF61-16C1-11D7-8645000102C1865D.
- MOSCARDELLI, L., and WOOD, L.J., 2015, Morphometry of mass-transport deposits as a predictive tool: *Geological Society of America Bulletin*, v. 128, p. B31221.1, doi: 10.1130/B31221.1.
- MUTTI, E., 1985, Turbidite systems and their relations to depositional sequences, in Zuffa, G.G., ed., *Provenance of Arenites*: D. Reidel Publishing Company, Cosenza, p. 65–93.
- MUTTI, E., BERNOULLI, D., RICCI, F., and TINTERRI, R., 2009, Turbidites and turbidity currents from Alpine ‘ flysch ’ to the exploration of continental margins: *Sedimentology*, v. 56, p. 267–318, doi: 10.1111/j.1365-3091.2008.01019.x.
- MUTTI, E., and NORMARK, W.R., 1987, Comparing Examples of Modern and Ancient Turbidite Systems: Problems and Concepts, in Leggett, J.K. and Zuffa, G.G., eds., *Marine Clastic Sedimentology: Concepts and Case Studies*: Springer Netherlands, Dordrecht, p. 1–38.
- MUTTI, E., and RICCI-LUCCHI, F., 1978, Turbidites of the northern Apennines: introduction to facies analysis: *International Geology Review*, v. 20, p. 125–166.
- MUTTI, E., TINTERRI, R., BENEVELLI, G., BIASE, D. di, and CAVANNA, G., 2003, Deltaic, mixed and turbidite sedimentation of ancient foreland basins: *Marine and Petroleum Geology*, v. 20, p. 733–755, doi: 10.1016/j.marpetgeo.2003.09.001.
- NALLY, D.V., 1996, A stratigraphic and sedimentologic analysis of a Lower Atoka sandstone, frontal Ouachita Thrustbelt, western Arkansas, in *Transactions of the 1995 AAPG Mid-Continent Section Meeting*: Tulsa Geological Society, Tulsa, Oklahoma, p. 74–83.
- NELSON, K.D., LILLIE, R.J., VOOGD, B. de, BREWER, J.A., OLIVER, J.E., KAUFMAN, S., BROWN, L., and VIELE, G.W., 1982, COCORP seismic reflection

- profiling in the Ouachita Mountains of western Arkansas: Geometry and geologic interpretation: *Tectonics*, v. 1, p. 413–430, doi: 10.1029/TC001i005p00413.
- NIEM, A.R., 1976, Patterns of Flysch Deposition and Deep-sea Fans in the Lower Stanley Group (Mississippian), Ouachita Mountains, Oklahoma and Arkansas: *Journal of Sedimentary Petrology*, v. 46, p. 633–646.
- NILSEN, T., SHEW, R.D., STEFFENS, G.S., and STUDLICK, J.R.J. (eds.), 2007, AAPG Studies in Geology 56: Atlas of Deep-Water Outcrops: American Association of Petroleum Geologists, Shell Exploration & Exploration, Tulsa, Oklahoma, 504 p.
- NORMARK, W.R., POSAMENTIER, H.W., and MUTTI, E., 1993, Turbidite systems: state of the art and future directions: *Review of Geophysics*, v. 31, p. 91–116.
- OAKES, M.C., 1953, Krebs and Cabaniss Groups of Pennsylvanian Age in Oklahoma: *American Association of Petroleum Geologists Bulletin*, v. 37, p. 1523–1526, doi: 10.1306/5CEADD37-16BB-11D7-8645000102C1865D.
- OLARIU, M.I., AIKEN, C.L. V., BHATTACHARYA, J.P., and XU, X., 2011, Interpretation of channelized architecture using three-dimensional photo real models, Pennsylvanian deep-water deposits at Big Rock Quarry, Arkansas: *Marine and Petroleum Geology*, v. 28, p. 1157–1170, doi: 10.1016/j.marpetgeo.2010.12.007.
- OLSZEWSKI, T.D., and PATZKOWSKY, M.E., 2003, From Cyclothems to Sequences: The Record of Eustasy and Climate on an Icehouse Epeiric Platform (Pennsylvanian-Permian, North American Midcontinent): *Journal of Sedimentary Research*, v. 73, p. 15–30, doi: 10.1306/061002730015.
- PAULI, D., 1994, Friable submarine channel sandstones in the Jackfork Group, Lynn Mountain Syncline, Pushmataha and Le Flore counties, Oklahoma, in Suneson, N.H. and Hemish, L.A., eds., *Geology and Resources of the Eastern Ouachita Mountains Frontal Belt and Southeastern Arkoma Basin, Oklahoma*: Oklahoma Geological Survey Guidebook 29: Oklahoma Geological Survey, Norman, Oklahoma, p. 179–202.
- PERRY, W.J.J., 1995, Arkoma Basin Province (062), in Gautier, D.L., Dolton, G.L., Takahashi, K.I., and Varnes, K.L., eds., *National Assessment of United States Oil and Gas Resources--Results, Methodology, and Supporting Data*: United States Geological Survey, Denver, p. 1–17.
- PETTINGA, L., JOBE, Z., SHUMAKER, L., and HOWES, N., 2018, Morphometric scaling relationships in submarine channel-lobe systems: *Geology*, v. 46, p. 819–822, doi: 10.1130/G45142.1.
- PICKERING, K.T., and HISCOTT, R.N., 2016, *Deep Marine Systems: Processes, Deposits, Environments, Tectonics and Sedimentation*: American Geophysical Union & Wiley, Chichester, West Sussex, UK; Hoboken, NJ, 657 p.
- PINTER, P.R., BUTLER, R.W.H., HARTLEY, A.J., MANISCALCO, R., BALDASSINI, N., and STEFANO, A. Di, 2016, The Numidian of Sicily revisited: a thrust-influenced

- confined turbidite system: *Marine*, v. 78, p. 291–311, doi: 10.1016/j.marpetgeo.2016.09.014.
- PINTER, P.R., BUTLER, R.W.H., HARTLEY, A.J., MANISCALCO, R., BALDASSINI, N., and DI STEFANO, A., 2018, Tracking sand-fairways through a deformed turbidite system: the Numidian (Miocene) of Central Sicily, Italy: *Basin Research*, v. 30, p. 480–501, doi: 10.1111/bre.12261.
- PRATHER, B.E., KELLER, F.B., and CHAPIN, M.A., 2000, Hierarchy of deep-water architectural elements with reference to seismic resolution: implications for reservoir prediction and modeling, in Weimer, P., Slatt, R.M., Coleman, J.L., Rosen, N.C., Nelson, C.H., Bouma, A.H., Styzen, M.J., and Lawrence, D.T., eds., GCSSEPM Foundation 20th Annual Research Conference, Deep-Water Reservoirs of the World: Gulf Coast Section Society of Economic Paleontologists and Mineralogists Foundation, Houston, TX, p. 817–835.
- PRÉLAT, A., HODGSON, D.M., and FLINT, S.S., 2009, Evolution, architecture and hierarchy of distributary deep-water deposits: a high-resolution outcrop investigation from the Permian Karoo Basin, South Africa: *Sedimentology*, v. 56, p. 2132–2154, doi: 10.1111/j.1365-3091.2009.01073.x.
- PUIGDEFÀBREGAS, C., MUÑOZ, J.A., and MARZO, M., 1986, Thrust Belt Development in the Eastern Pyrenees and Related Depositional Sequences in the Southern Foreland Basin, in Allen, P.A. and Homewood, P., eds., *Foreland Basins - International Association of Sedimentologists Special Publication No. 8*: Wiley-Blackwell, Oxford; London; Edinburgh; Boston; Palo Alto; Melbourne, p. 229–249.
- PYLES, D.R., 2007, Architectural Elements in a Ponded Submarine Fan, Carboniferous Ross Sandstone, Western Ireland, in Nilsen, T.H., Shew, R.D., Steffens, G.S., and Studlick, J.R., eds., *Atlas of Deep-Water Outcrops: AAPG Studies in Geology 56 CD-ROM*: American Association of Petroleum Geologists, Tulsa, Oklahoma, p. 1–19.
- PYLES, D.R., JENNETTE, D., KENDALL, C., MCCAF, B., MARTINSEN, O.J., SULLIVAN, M., KRAUS, M., PULHAM, A., ABREU, V., WAGONER, J. Van, CAMPION, K., DUNN, P., SULLIVAN, M., MAGEE, G., et al., 2008, Multiscale stratigraphic analysis of a structurally confined submarine fan: Carboniferous Ross Sandstone, Ireland: *American Association of Petroleum Geologists Bulletin*, v. 92, p. 557–587, doi: 10.1306/01110807042.
- RAVNÅS, R., and STEEL, R.J., 1998, Architecture of Marine Rift-Basin Successions: *American Association of Petroleum Geologists Bulletin*, v. 82, p. 110–146, doi: 10.1306/1D9BC3A9-172D-11D7-8645000102C1865D.
- REMACHA, E., FERNA, L.P., and FERNÁNDEZ, L.P., 2003, High-resolution correlation patterns in the turbidite systems of the Hecho Group (South-Central Pyrenees, Spain): *Marine and Petroleum Geology*, v. 20, p. 711–726, doi: 10.1016/j.marpetgeo.2003.09.003.

- RICCI-LUCCHI, F., 1986, The Oligocene to Recent Foreland Basins of the Northern Apennines, in Allen, P.A. and Homewood, P., eds., *Foreland Basins - International Association of Sedimentologists Special Publication No. 8*: Wiley-Blackwell, Oxford; London; Edinburgh; Boston; Palo Alto; Melbourne, p. 103–139.
- RICCI-LUCCHI, F., 2003, Turbidites and foreland basins: an Apenninic perspective: *Marine and Petroleum Geology*, v. 20, p. 727–732, doi: 10.1016/j.marpetgeo.2003.02.003.
- RIEKE, H.H., and KIRR, J.N., 1984, Geologic overview, coal and coalbed methane resources of the Arkoma Basin, Arkansas and Oklahoma, in Rightmire, C.T., Eddy, G.E., and Kirr, J.N., eds., *Coalbed Methane Resources of the United States (AAPG Studies in Geology Volume 17)*: American Association of Petroleum Geologists, Tulsa, Oklahoma, p. 135–161.
- ROMANS, B.W., FILDANI, A., HUBBARD, S.M., COVAULT, J.A., FOSDICK, J.C., and GRAHAM, S.A., 2011, Evolution of deep-water stratigraphic architecture, Magallanes Basin, Chile: *Marine and Petroleum Geology*, v. 28, p. 612–628, doi: 10.1016/j.marpetgeo.2010.05.002.
- ROMANS, B.W., HUBBARD, S.M., and GRAHAM, S.A., 2009, Stratigraphic evolution of an outcropping continental slope system, Tres Pasos Formation at Cerro Divisadero, Chile: *Sedimentology*, v. 56, p. 737–764, doi: 10.1111/j.1365-3091.2008.00995.x.
- SALEH, A., 2004, *Correlation of Atoka and Adjacent Strata Within a Sequence Stratigraphic Framework, Arkoma Basin, Oklahoma*: University of Oklahoma, 188 p.
- SALLES, L., FORD, M., and JOSEPH, P., 2014, Characteristics of axially-sourced turbidite sedimentation on an active wedge-top basin (Annot Sandstone, SE France): *Marine and Petroleum Geology*, v. 56, p. 305–323, doi: 10.1016/j.marpetgeo.2014.01.020.
- SGAVETTI, M., 1991, Photostratigraphy of Ancient Turbidite Systems, in Weimer, P. and Link, M.H., eds., *Seismic Facies and Sedimentary Processes of Submarine Fans and Turbidite Systems. Frontiers in Sedimentary Geology*: Springer, New York, NY, p. 107–125.
- SHARMAN, G.R., HUBBARD, S.M., COVAULT, J.A., HINSCH, R., LINZER, H.-G., and GRAHAM, S.A., 2018, Sediment routing evolution in the North Alpine Foreland Basin, Austria: interplay of transverse and longitudinal sediment dispersal: *Basin Research*, v. 30, p. 426–447, doi: 10.1111/bre12259.
- SHARRAH, K.L., 2006, *Comparative Study and Provenance of the Atoka Formation in the Frontal Ouachita Thrust Belt, Oklahoma*: University of Tulsa, 268 p.
- SHAULIS, B.J., LAPEN, T.J., CASEY, J.F., and REID, D.R., 2012, Timing and rates of flysch sedimentation in the Stanley Group, Ouachita Mountains, Oklahoma and Arkansas, U.S.A.: Constraints from U-Pb zircon ages of subaqueous ash-flow tuffs: *Journal of Sedimentary Research*, v. 82, p. 833–840.

- SHIDELER, G.L., 1970, Provenance of Johns Valley Boulders in Late Paleozoic Ouachita Facies, Southeastern Oklahoma and Southwestern Arkansas: *American Association of Petroleum Geologists Bulletin*, v. 5, p. 789–806.
- SHUMAKER, L.E., JOBE, Z.R., JOHNSTONE, S.A., PETTINGA, L.A., CAI, D., and MOODY, J.D., 2018, Controls on submarine channel-modifying processes identified through morphometric scaling relationships: *Geosphere*, v. 14, p. 2171–2187, doi: 10.1130/GES01674.1.
- SINCLAIR, H.D., 2012, Thrust wedge/foreland basin systems, in Busby, C. and Azor, A., eds., *Tectonics of Sedimentary Basins: Recent Advances*: Wiley-Blackwell, Oxford; Chichester; Hoboken, p. 522–537.
- SLATT, R.M., and STONE, C.G., 2001, Deepwater (turbidite) sandstone elements of the Jackfork Group in Arkansas: application to exploration and development in eastern Oklahoma: *The Shale Shaker*, v. 51, p. 93–101.
- SLATT, R.M., STONE, C.G., and WEIMER, P., 2000, Characterization of slope and basin facies tracts, Jackfork Group, Arkansas, with applications to deepwater (turbidite) reservoir management, in Weimer, P., Slatt, R.M., Coleman, J.L., Rosen, Norman, C., Nelson, C.H., Bouma, A.H., Styzen, M.J., and Lawrence, D.T., eds., *GCSSEPM Foundation 20th Annual Research Conference, Deep-Water Reservoirs of the World: Gulf Coast Section Society of Economic Paleontologists and Mineralogists Foundation*, Houston, TX, p. 940–980.
- SØMME, T.O., SKOGSEID, J., EMBRY, P., LØSETH, H., and VAL, P., 2019, Manifestation of Tectonic and Climatic Perturbations in Deep-Time Stratigraphy – An Example From the Paleocene Succession Offshore Western Norway: *Frontiers in Earth Science*, v. 7, p. 1–20, doi: 10.3389/feart.2019.00303.
- SPRAGUE, A.R.G., 1985, Depositional environment and petrology of the lower member of the Pennsylvanian Atoka Formation, Ouachita Mountains, Arkansas and Oklahoma: *The University of Texas at Dallas*, 587 p.
- SPYCHALA, Y.T., HODGSON, D.M., PRÉLAT, A., KANE, I.A., FLINT, S.S., and MOUNTNEY, N.P., 2017, Frontal and Lateral Submarine Lobe Fringes: Comparing Sedimentary Facies, Architecture and Flow Processes: *Journal of Sedimentary Research*, v. 87, p. 75–96, doi: 10.2110/jsr.2017.2.
- STARK, P.H., 1966, Stratigraphy and environment of deposition of the Atoka Formation in the Central Ouachita Mountains, Oklahoma, in *Flysch Facies and Structure of the Ouachita Mountains: Guidebook, 29th Field Conference*: Oklahoma Geological Survey, Norman, Oklahoma, p. 164–176.
- STOW, D.A. V., and TABREZ, A.R., 2002, Quaternary sedimentation on the Makran margin: turbidity current-hemipelagic interaction in an active slope-apron system: *Geological Society, London, Special Publications*, v. 1, p. 195, 219–236, doi: 10.1144/GSL.SP.2002.195.01.12.

- STRAUB, K.M., PAOLA, C., MOHRIG, D., WOLINSKY, M. a., and GEORGE, T., 2009, Compensational Stacking of Channelized Sedimentary Deposits: *Journal of Sedimentary Research*, v. 79, p. 673–688, doi: 10.2110/jsr.2009.070.
- SUNESON, N.H., 2012, Arkoma Basin petroleum: past, present, and future: *Shale Shaker Digest*, v. 63, p. 38–70.
- SUNESON, N.H. (ed.), 2008, Stratigraphic and structural evolution of the Ouachita Mountains and Arkoma Basin, southeastern Oklahoma and west-central Arkansas: applications to petroleum exploration: 2004 field symposium (the Arbenz-Misch/Oles Volume): Oklahoma Geological Survey, Norman, Oklahoma, 92 p.
- SUNESON, N.H., and FERGUSON, C.A., 1987, Ouachita Mountains frontal belt field trip. Oklahoma Geological Survey OF-87: Oklahoma Geological Survey, Norman, Oklahoma, 40 p.
- SUTCLIFFE, C., and PICKERING, K.T., 2009, End-signature of deep-marine basin-fill, as a structurally confined low-gradient clastic system: the Middle Eocene Guaso system, South-central Spanish Pyrenees: *Sedimentology*, v. 56, p. 1670–1689, doi: 10.1111/j.1365-3091.2009.01051.x.
- SUTHERLAND, P.K., 1982, Lower and Middle Pennsylvanian Stratigraphy in South-Central Oklahoma. Oklahoma Geological Survey Guidebook 20.:
- SYLVESTER, Z., 2007, Turbidite bed thickness distributions: methods and pitfalls of analysis and modeling: *Sedimentology*, v. 54, p. 847–870, doi: 10.1111/j.1365-3091.2007.00863.x.
- TAGLIAFERRI, A., and TINTERRI, R., 2016, The tectonically confined Firenzuola turbidite system (Marnoso-Arenacea Formation, northern Apennines, Italy): *Italian Journal of Geosciences*, v. 135, p. 425–443, doi: 10.3301/IJG.2015.27.
- TERLAKY, V., WILLIAM, R., and ARNOTT, C., 2016, The Control Of Terminal-Splay Sedimentation On Depositional Patterns and Stratigraphic Evolution In Avulsion-Dominated, Unconfined, Deep-Marine Basin-Floor Systems: *Journal of Sedimentary Research*, v. 86, p. 786–799, doi: 10.2110/jsr.2016.51.
- THOMAS, W.A., 2011, Detrital-zircon geochronology and sedimentary provenance: *Lithosphere*, v. 3, p. 304–308, doi: 10.1130/rlf.1001.1.
- THOMAS, W.A., 1976, Evolution of Ouachita-Appalachian continental margin: *The Journal of Geology*, v. 84, p. 323–342.
- THOMAS, W.A., 2004, Genetic relationship of rift-stage crustal structure, terrane accretion, and foreland tectonics along the southern Appalachian-Ouachita orogen: *Journal of Geodynamics*, v. 37, p. 549–563, doi: 10.1016/j.jog.2004.02.020.
- THOMAS, W.A., 1997, Nd isotopic constraints on sediment sources of the Ouachita-Marathon fold belt : Alternative Interpretation and Reply Alternative Interpretation:

- Geological Society of America Bulletin, v. 109, p. 1192–1210, doi: 10.1130/0016-7606(1997)109<0779.
- THOMAS, W.A., GEHRELS, G.E., LAWTON, T.F., SATTERFIELD, J.I., ROMERO, M.C., and SUNDELL, K.E., 2019, Detrital zircons and sediment dispersal from the Coahuila terrane of northern Mexico into the Marathon foreland of the southern Midcontinent: *Geosphere*, v. 15, p. 1–26, doi: 10.1130/GES02033.1/4785836/ges02033.pdf.
- TINTERRI, R., LAPORTA, M., and OGATA, K., 2017, Asymmetrical cross-current turbidite facies tract in a structurally-confined mini-basin (Priabonian-Rupelian, Ranzano Sandstone, northern Apennines, Italy): *Sedimentary Geology*, v. 352, p. 63–87, doi: 10.1016/j.sedgeo.2016.12.005.
- TINTERRI, R., and TAGLIAFERRI, A., 2015, The syntectonic evolution of foredeep turbidites related to basin segmentation: Facies response to the increase in tectonic confinement (Marnoso-Arenacea Formation, Miocene, Northern Apennines, Italy): *Marine and Petroleum Geology*, v. 67, p. 81–110, doi: 10.1016/j.marpetgeo.2015.04.006.
- VIELE, G.W., 1979, Geologic map and cross section, eastern Ouachita Mountains, Arkansas: Map summary: *Geological Society of America Bulletin*, v. 90, p. 1096–1099.
- VIELE, G.W., 1966, The regional structure of the Ouachita Mountains of Arkansas, a hypothesis, in Cline, L.M., ed., *Flysch Facies and Structure of the Ouachita Mountains: Guidebook, 29th Field Conference*: Kansas Geological Society, Lawrence, KS, p. 245–278.
- VIELE, G.W., and THOMAS, W.A., 1989, Tectonic synthesis of the Ouachita orogenic belt, in Hatcher, R.D., Thomas, W.A., and Viele, G.W., eds., *The Appalachian-Ouachita Orogen in the United States*: Geological Society of America, Norman, Oklahoma, Oklahoma, p. 695–728.
- VINNELS, J.S., BUTLER, R.W.H., CAFFREY, W.D., and LICKORISH, W.H., 2010, Sediment Distribution and Architecture Around a Bathymetrically Complex Basin: An Example from the Eastern Champsaur Basin, Se France: *Journal of Sedimentary Research*, v. 80, p. 216–235, doi: 10.2110/jsr.2010.025.
- WALKER, R.G., 1978, Deep-Water Sandstone Facies and Ancient Submarine Fans: Models for Exploration for Stratigraphic Traps: *American Association of Petroleum Geologists Bulletin*, v. 62, p. 932–966, doi: 10.1306/C1EA4F77-16C9-11D7-8645000102C1865D.
- WALTHALL, B.H., 1967, Stratigraphy and Structure, Part of Athens Plateau, Southern Ouachitas, Arkansas: *American Association of Petroleum Geologists Bulletin*, v. 51, p. 120, doi: 10.1306/5D25C0A1-16C1-11D7-8645000102C1865D.

- WANG, X., LUTHI, S.M., HODGSON, D.M., SOKOUTIS, D., WILLINGSHOFER, E., and GROENENBERG, R.M., 2017, Turbidite stacking patterns in salt-controlled minibasins: Insights from integrated analogue models and numerical fluid flow simulations: *Sedimentology*, v. 64, p. 530–552, doi: 10.1111/sed.12313.
- WUELLNER, D.E., LEHTONEN, L.R., and JAMES, W.C., 1986, Sedimentary-Tectonic Development of the Marathon and Val Verde Basins, West Texas, U.S.A.: A Permian–Carboniferous Migrating Foredeep, in Allen, P.A. and Homewood, P., eds., *Foreland Basins - International Association of Sedimentologists Special Publication No. 8*: Wiley-Blackwell, Oxford; London; Edinburgh; Boston; Palo Alto; Melbourne, p. 347–368.
- WYNN, R.B., TALLING, P.J., MASSON, D.G., LE BAS, T.P., CRONIN, B.T., and STEVENSON, C.J., 2012, The influence of subtle gradient changes on deep-water gravity flows: a case study from the Moroccan turbidite system, in Prather, B.E., Deptuck, M.E., Mohrig, D., Van Hoorn, B., and Wynn, R.B., eds., *Application of the Principles of Seismic Geomorphology to Continental-Slope and Base-of-Slope Systems: Case Studies from Seafloor and Near-Seafloor Analogues*. SEPM Special Publication No. 99: SEPM (Society for Sedimentary Geology), Tulsa, p. 145–161.
- XU, C., CRONIN, T.P., MCGUINNESS, T.E., and STEER, B., 2009, Middle Atokan sediment gravity flows in the Red Oak field, Arkoma Basin, Oklahoma: A sedimentary analysis using electrical borehole images and wireline logs: *American Association of Petroleum Geologists Bulletin*, v. 93, p. 1–29, doi: 10.1306/09030808054.
- ZACHRY, D.L., and SUTHERLAND, P.K., 1984, Stratigraphy and depositional framework of the Atoka Formation (Pennsylvanian), Arkoma Basin of Arkansas and Oklahoma: The Atokan Series (Pennsylvanian) and its boundaries: a symposium. *Oklahoma Geological Survey Bulletin*, v. 136, p. 9–17.
- ZOU, F., SLATT, R.M., BASTIDAS, R., and RAMIREZ, B., 2012, Integrated outcrop reservoir characterization, modeling, and simulation of the Jackfork Group at the Baumgartner Quarry area, western Arkansas: implications to Gulf of Mexico deep-water exploration and production: *American Association of Petroleum Geologists Bulletin*, v. 96, p. 1429–1448, doi: 10.1306/01021210146.
- ZOU, F., SLATT, R.M., ZHANG, J., and HUANG, T., 2017, An integrated chemo- and sequence-stratigraphic framework of the Early Pennsylvanian deepwater outcrops near Kirby, Arkansas, USA, and its implications on remnant basin tectonics: *Marine and Petroleum Geology*, v. 81, p. 252–277, doi: 10.1016/j.marpetgeo.2017.01.006.

FIGURES

TECTONIC-SEDIMENTARY INTERPLAY, OUACHITA MOUNTAINS

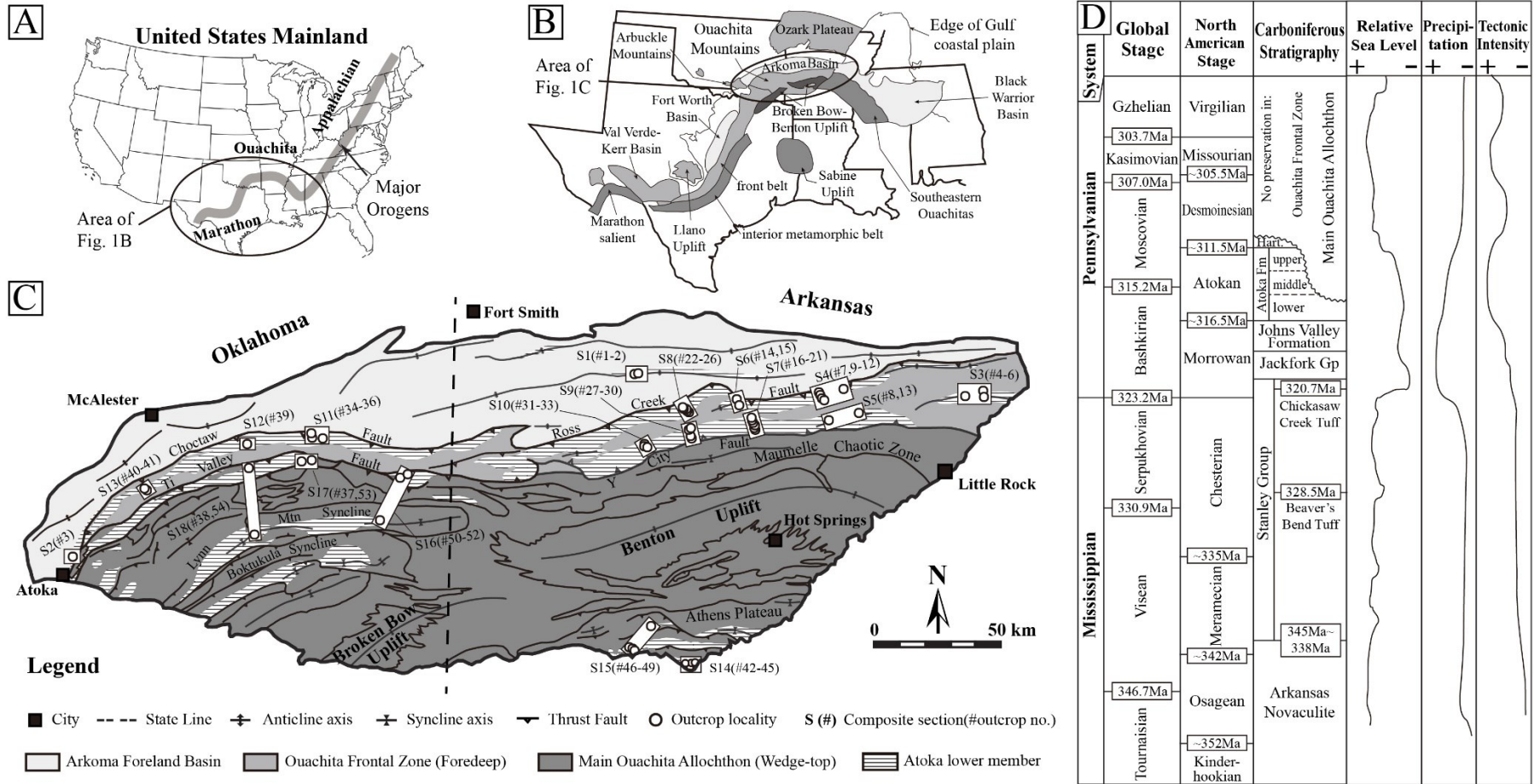


FIG. 1. – A: Location of the study area in the continental US. B: Simplified geologic map of southern midcontinent and the Gulf Coast showing the Ouachita and Marathon fold and thrust belts (after Golonka et al., 2007). C: Simplified geologic map of the Ouachita Mountains and Arkoma Basin showing the outcrop localities of the lower Atoka formation and the three structural-depositional zones: Arkoma Foreland Basin, Ouachita Frontal Zone (foredeep), and Main Ouachita Allochthon (wedge-top) (after Arbenz, 2008). Detailed information on the localities is listed in the supplementary dataset. D: Stratigraphy, relative sea level, precipitation, and tectonic intensity of the Carboniferous in the Ouachita Mountains (after Coleman, 2000; Heckel and Clayton, 2006; Suneson, 2012). ‘Hart’ for Hartshorne Formation.

TECTONIC-SEDIMENTARY INTERPLAY, OUACHITA MOUNTAINS

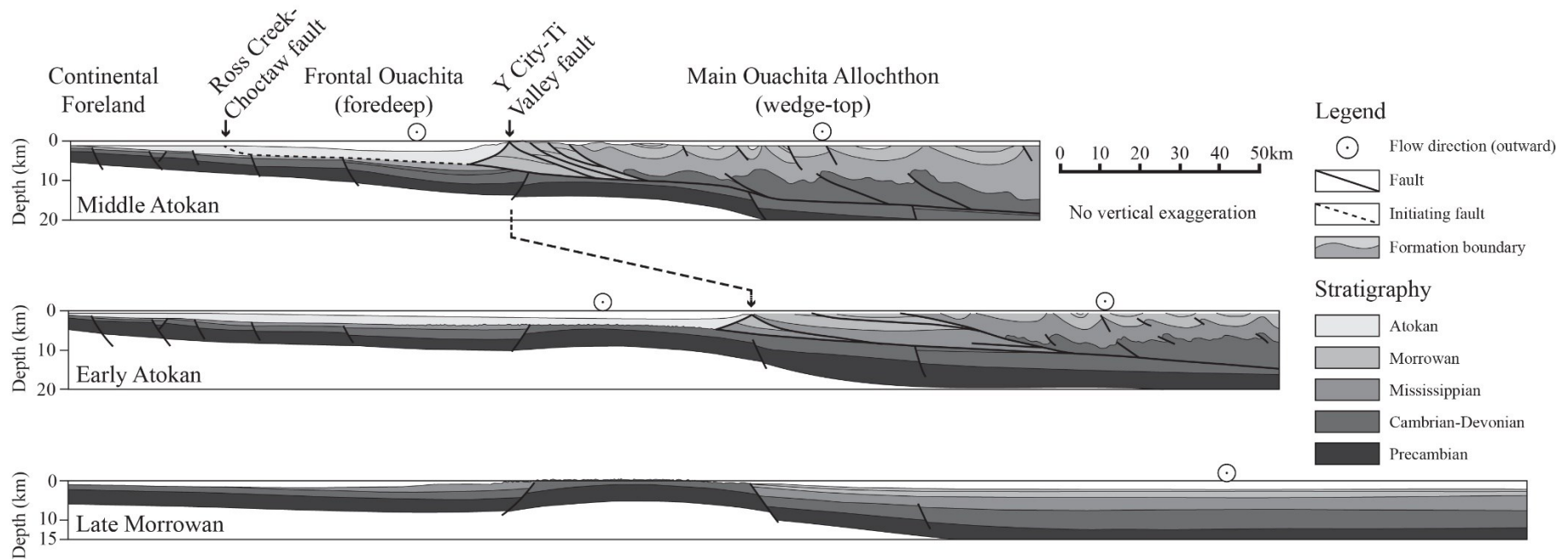


FIG. 2. – Structural evolution based on a geological cross-section of the Ouachita Mountains from Late Morrowan to Middle Atokan (Pennsylvanian), showing the contrasting structural styles of the Ouachita Frontal Zone and the Main Ouachita Allochthon (after Arbenz, 2008).

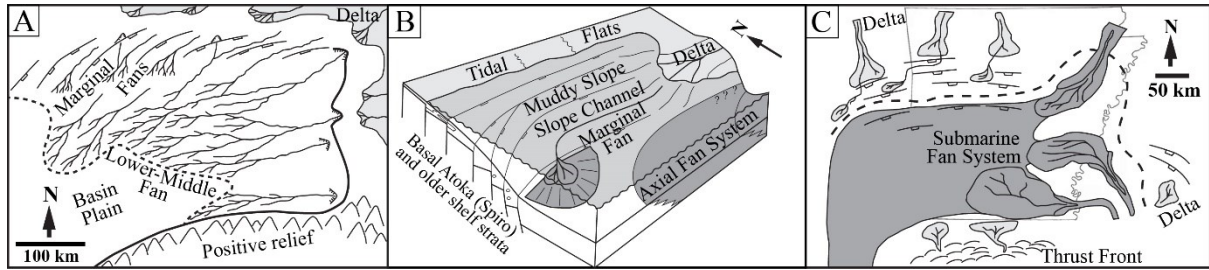


FIG. 3. – Depositional models proposed for the Pennsylvanian Atoka Formation in the Arkoma Basin and the Ouachita Mountains. A: a depositional model for the lower Atoka formation showing a predominant east-to-west sediment dispersal system (after Sprague, 1985); B: a depositional model for the Atoka Formation showing the co-existence of an axial fan and a slope (marginal) fan in the Arkoma Basin (after Houseknecht, 1986); C: synthesized depositional model showing the basin shape and potential sources (after Coleman, 2000).

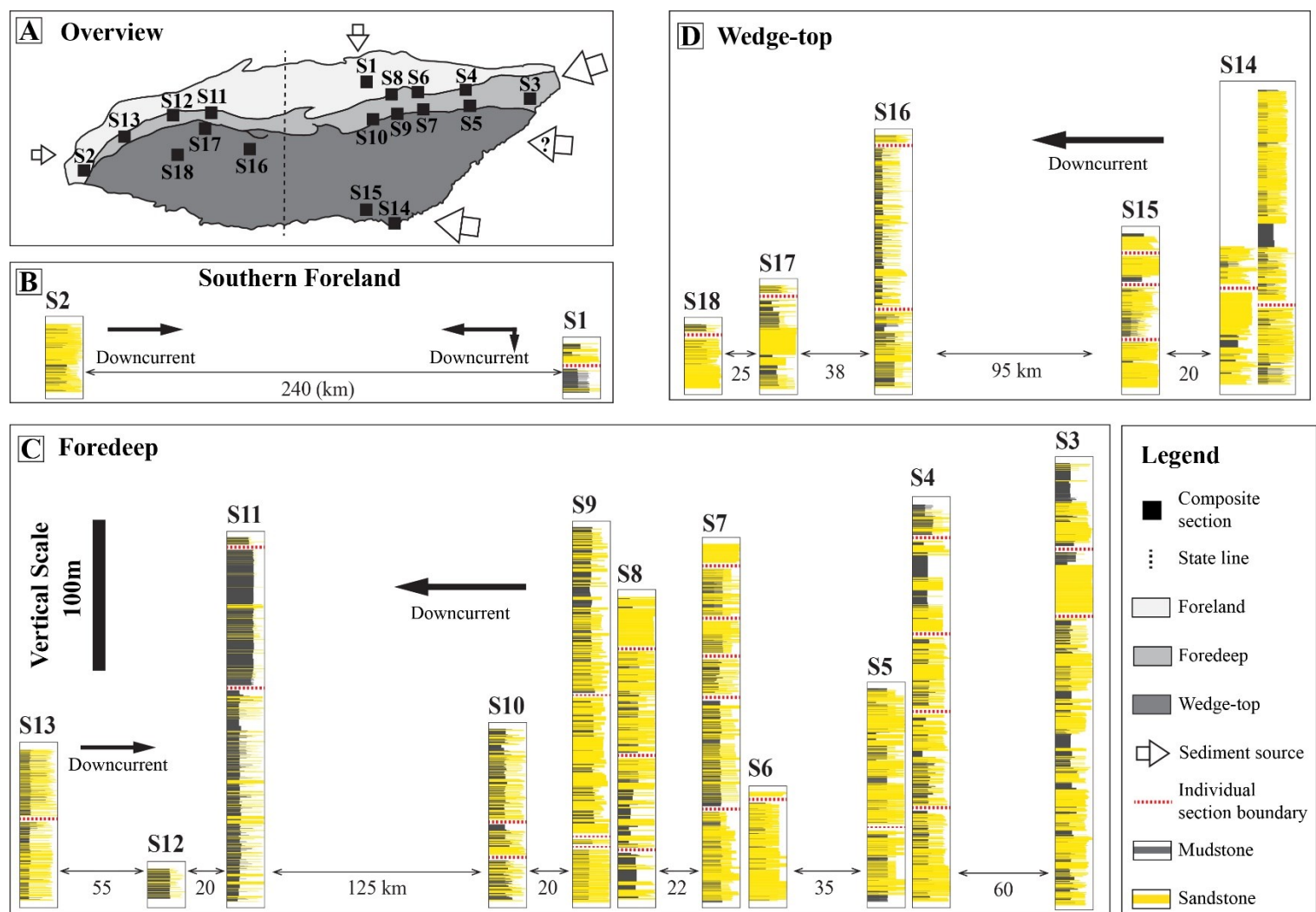


FIG. 4. – A: Overview map with composite section locations and sediment entry points. B-D: gross stratigraphic correlations of measured sections and general sediment transport directions of the lower Atoka formation in southern foreland, foredeep, and wedge-top, respectively. No datum or bed-by-bed correlations between sections is implied.

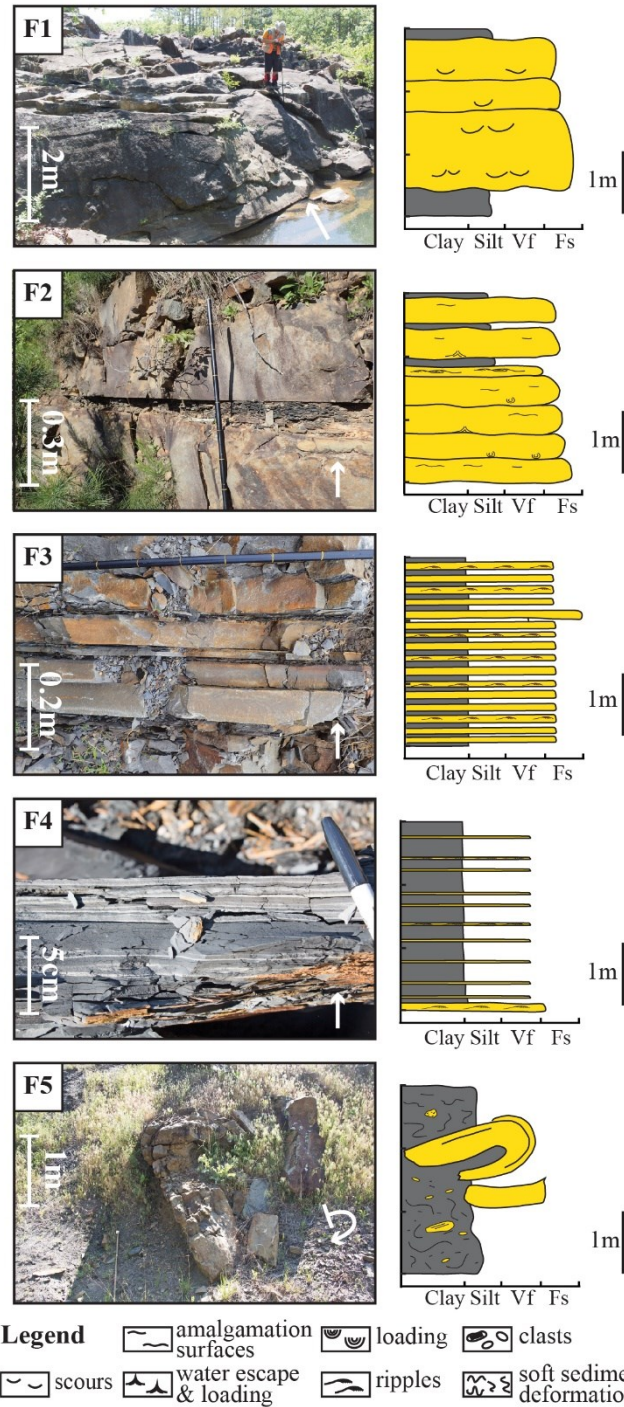


FIG. 5. – Lithofacies and idealized stratigraphic columns in this study. F1. Massive, amalgamated sandstone; F2. Thick-bedded sandstone with minor mudstone; F3. Thin-bedded sandstone and mudstone; F4. Mudstone with minor sandstone; F5. Disturbed mudstone and sandstone.

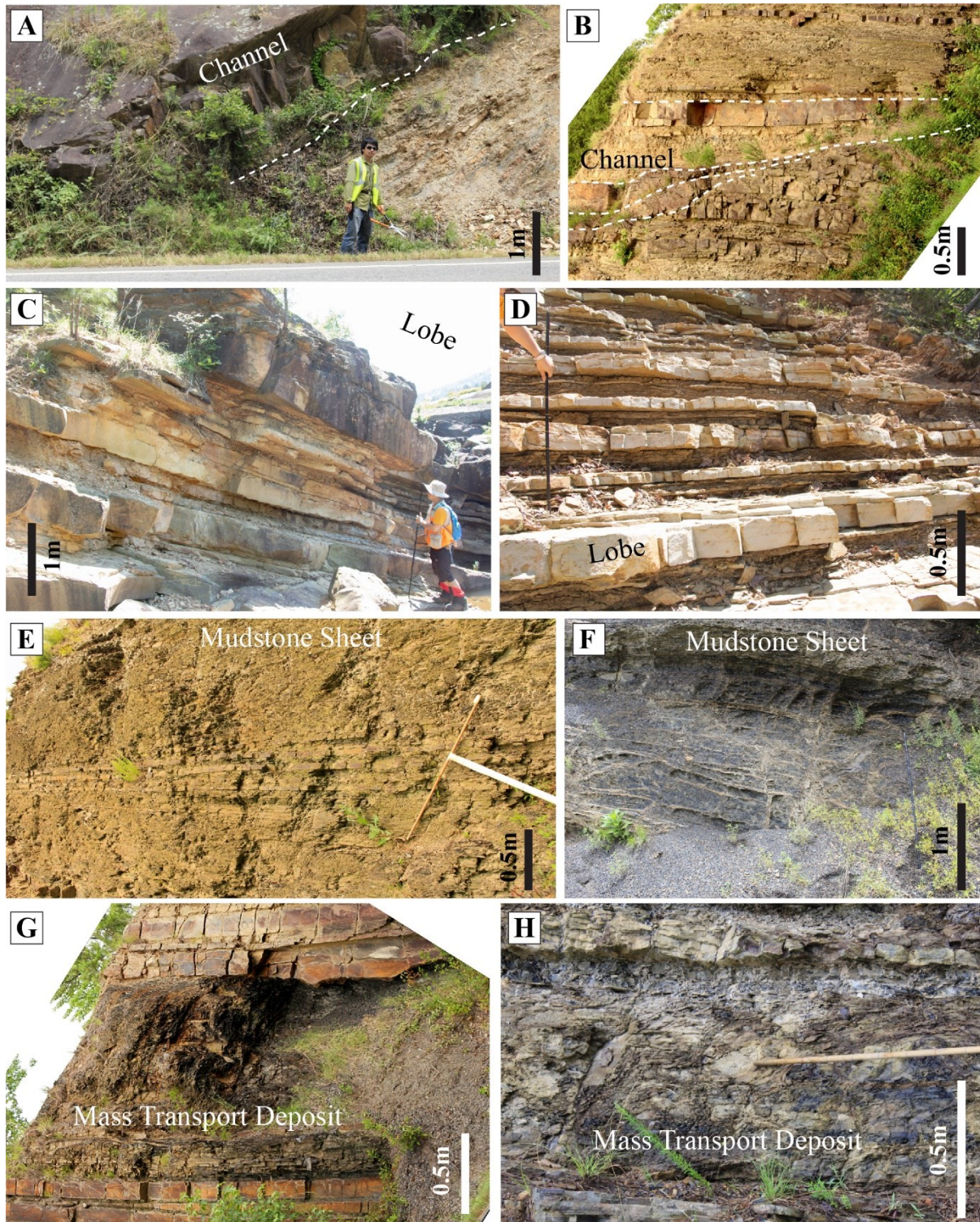


FIG. 6. – Outcrop examples of facies associations of the lower Atoka formation. A: FA1, channel filled with massive sandstones. B: FA1, channel filled with thin-bedded sandstone and mudstone. C: FA2, thick-bedded, sand-rich lobe. D: FA2, thin-bedded, mud-rich lobe. E: FA3, heterolithic mudstone sheet. F: FA3, clay-rich, laminated mudstone sheet. G: FA4, mudstone slump. H: FA4, mud-rich debris flow deposit.

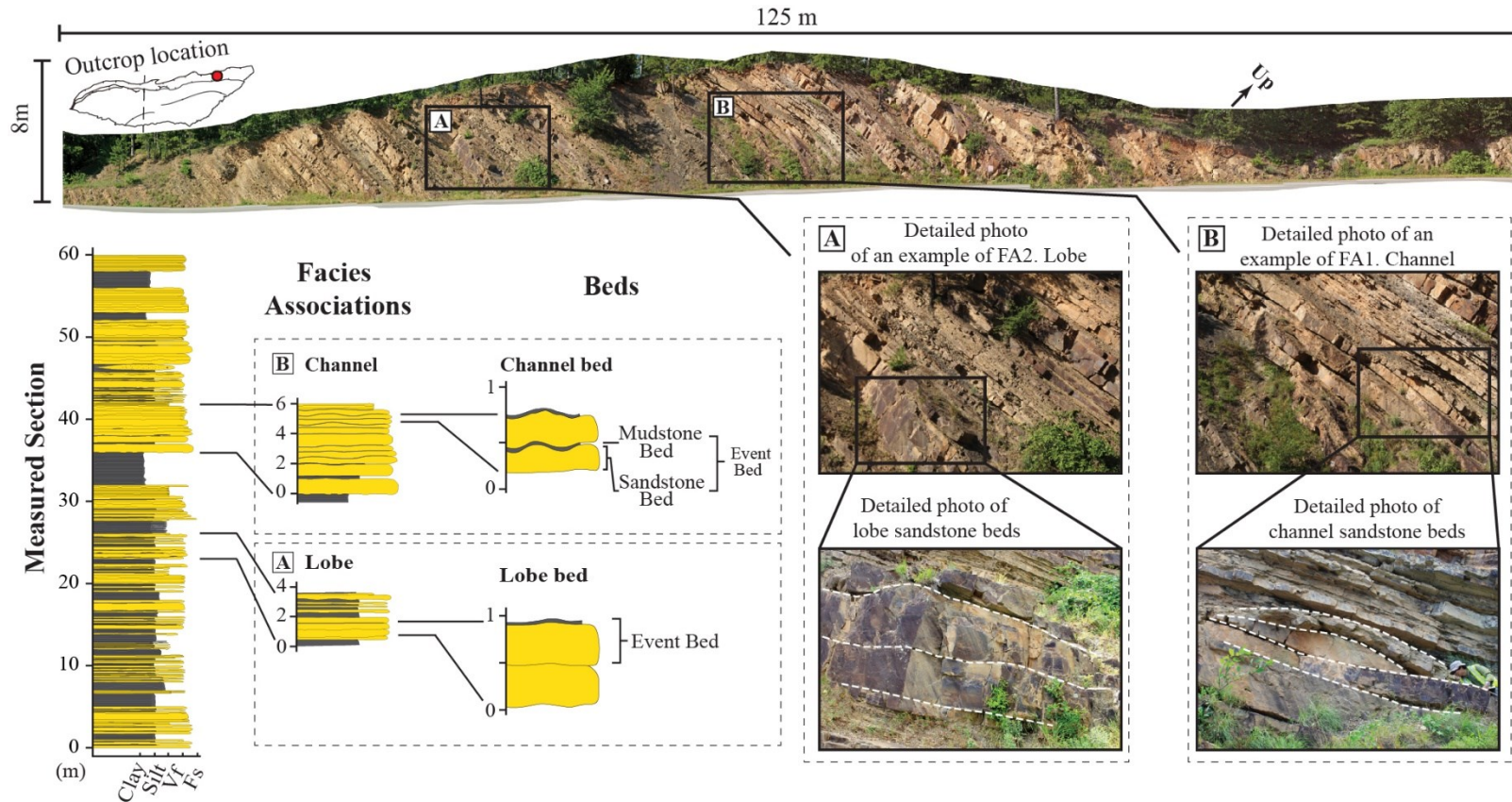


FIG. 7. – An example of an outcrop photo mosaic and the measured section showing the recognition of channel and lobe in this study. The outcrop is a roadcut at AR Highway 9/10 between Perry and Perryville in Perry County, Arkansas. Channels are distinguished from lobes by erosive surfaces at the base and variable thickness, geometry, and dipping of the sandstones within the outcrop extent.

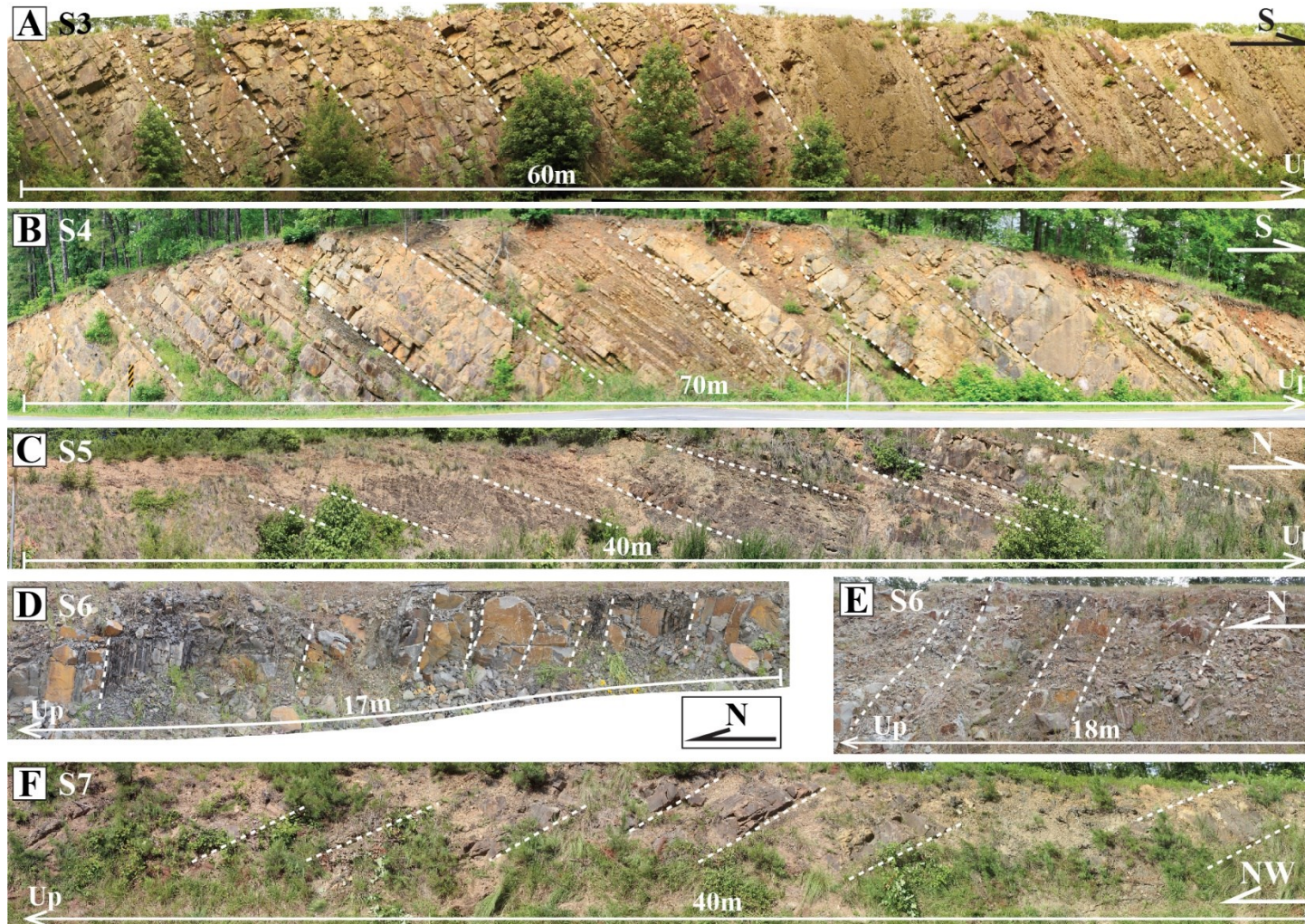


FIG. 8. – Representative outcrop photo panels of the foredeep, Part One. A. sand-rich lobe, mudstone sheet, and channel fill at S3 (Arkansas Hwy 5 near Jacksonville). B. sand-rich lobes and mudstone sheets at S4 (AR Hwy 9/10, between Perry and Perryville). C. heterolithic mudstone sheets and lobes at S5 (AR Hwy 9/10 north of Thornburg). D & E fresh roadcuts showing sand-rich lobes and mudstone sheets at S6 (Arkansas Hwy 7, south of Ola). Please see Table 5 for more descriptions.

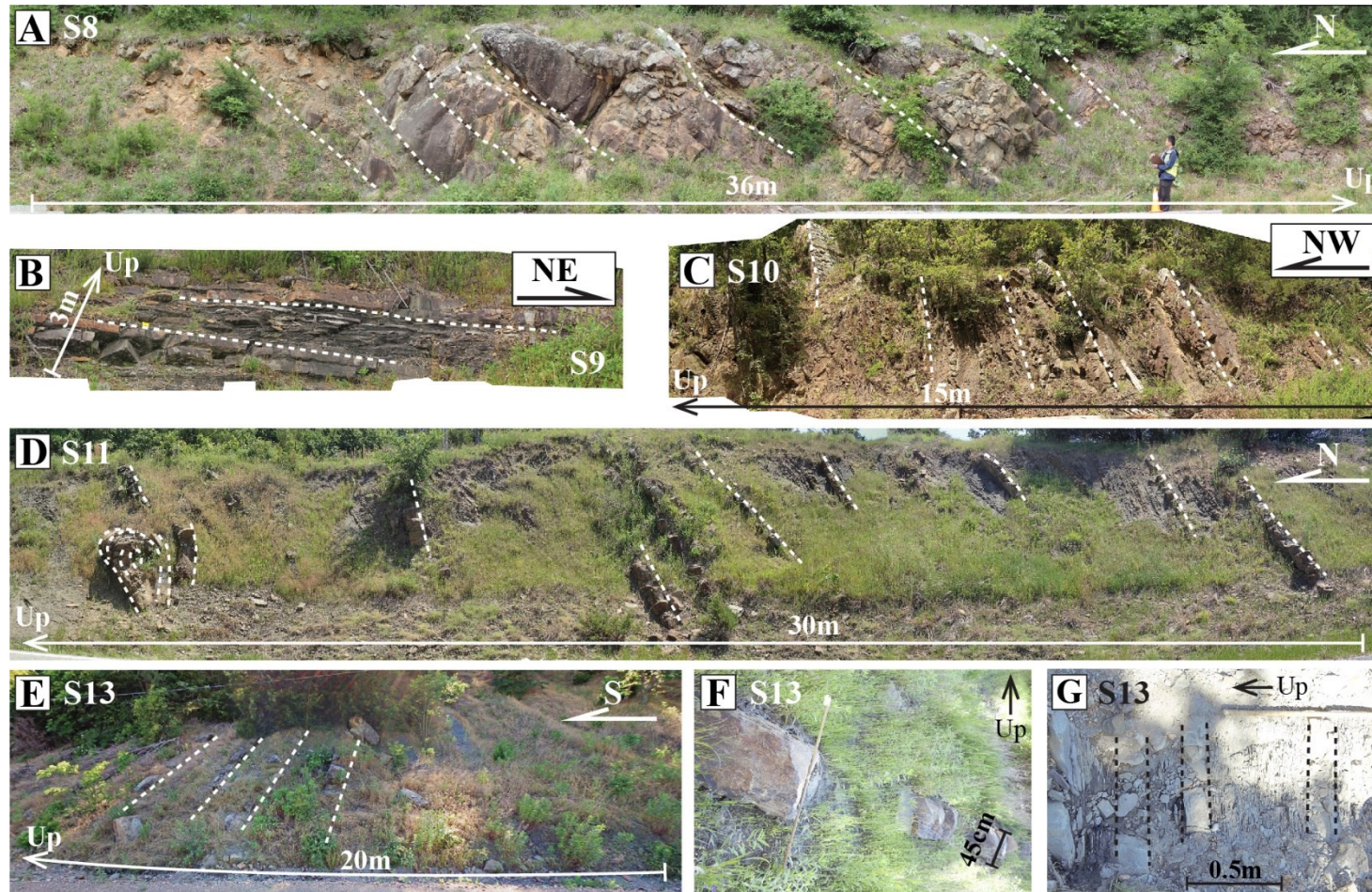


FIG. 9. – Representative outcrop photo panels of the foredeep, Part Two. A. amalgamated channel fills and sand-rich lobes at S8 (Arkansas Hwy 27, south of Danville). B. laminated and heterolithic mudstone sheets and mud-rich lobes at S9 (Arkansas Hwy 27, north of Onyx). C. laminated mudstone sheets and lobes at S10 (Chula, Arkansas). Outcrop beds are overturned. D. mudstone sheets with some slump deposits at S11 (Oklahoma Hwy 82, near Bengal). Outcrop beds are overturned. E, F, G. isolated lobes and thick heterolithic mudstone sheets at S13 (gravel road near Indian Nation Turnpike, Oklahoma, south of Blanco). No photo panel is available for S12. Please see Table 5 for more descriptions.

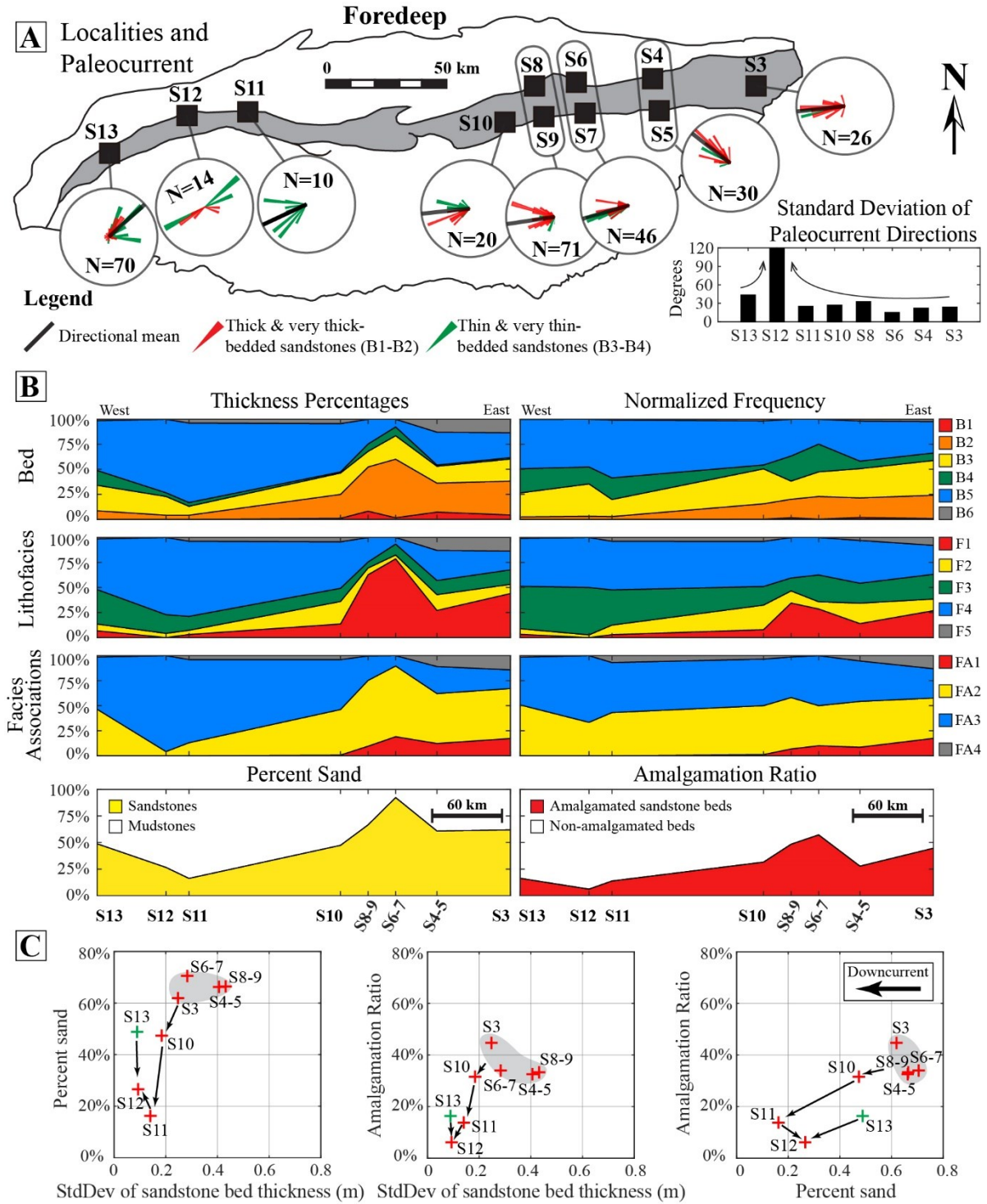


FIG. 10. – Facies distribution in the foredeep zone. A: locations of the composite sections, rose diagrams of paleocurrent directions, and standard deviations of the paleocurrent directions. B: longitudinal variations in thickness proportions and normalized frequency of the components in the facies hierarchy. C: scatter plots of the statistical parameters, i.e. percent sand, amalgamation ratio, and standard deviation of sandstone bed thickness, for each composite section. Red crosses represent the main west-prograding fan and green crosses represent the small east-prograding fan. The parameters overall decrease in downcurrent direction.

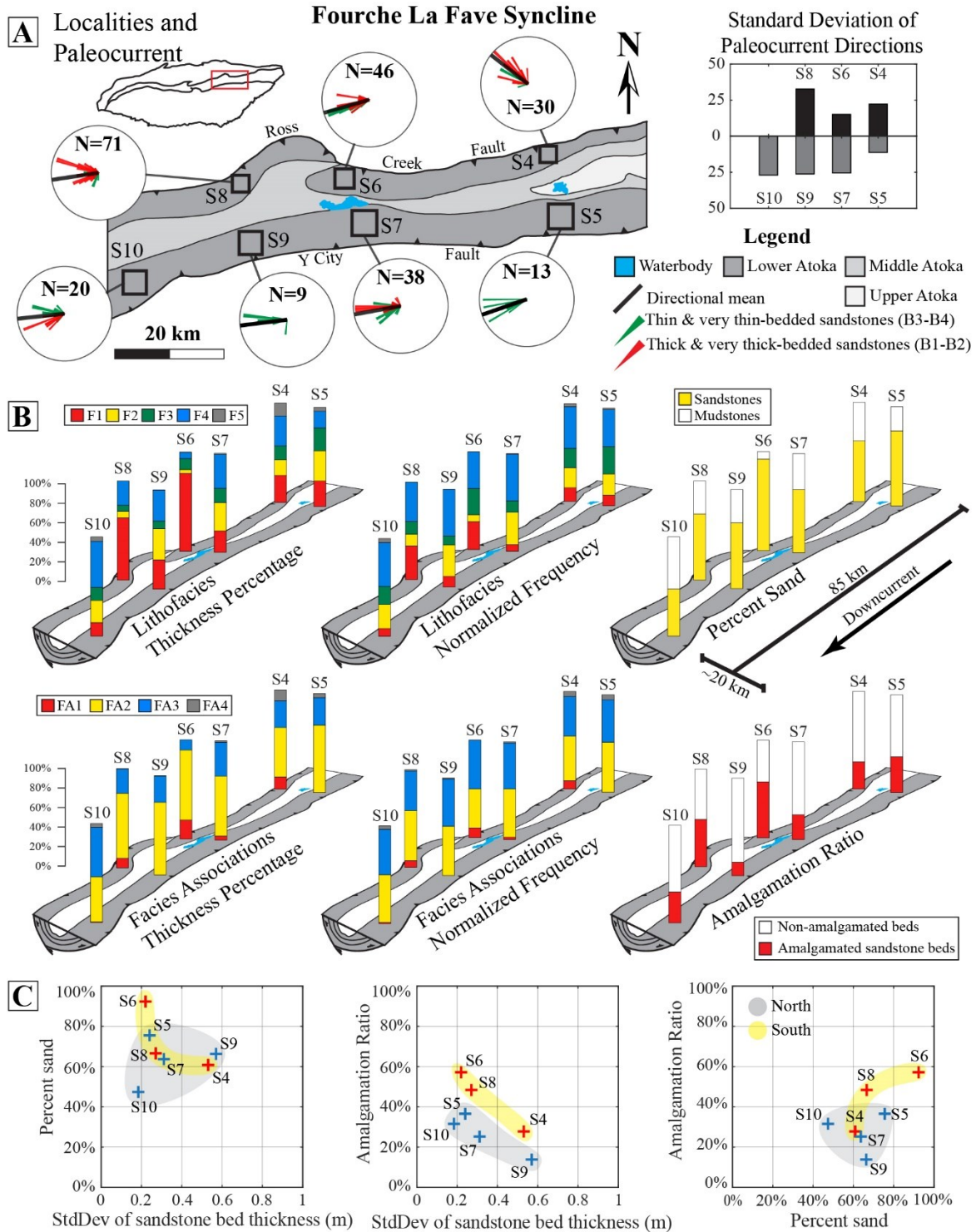


FIG. 11. – Facies distribution in Fourche La Fave Syncline in Arkansas showing asymmetrical facies distribution between the north and south limbs. A. both limbs show similar paleocurrent patterns. B. the north limb shows overall more sand-rich facies compositions. C. the north limb shows overall higher percent sand, amalgamation ratio, and variability in sandstone thickness. Red and blue crosses represent the north and south localities, respectively.

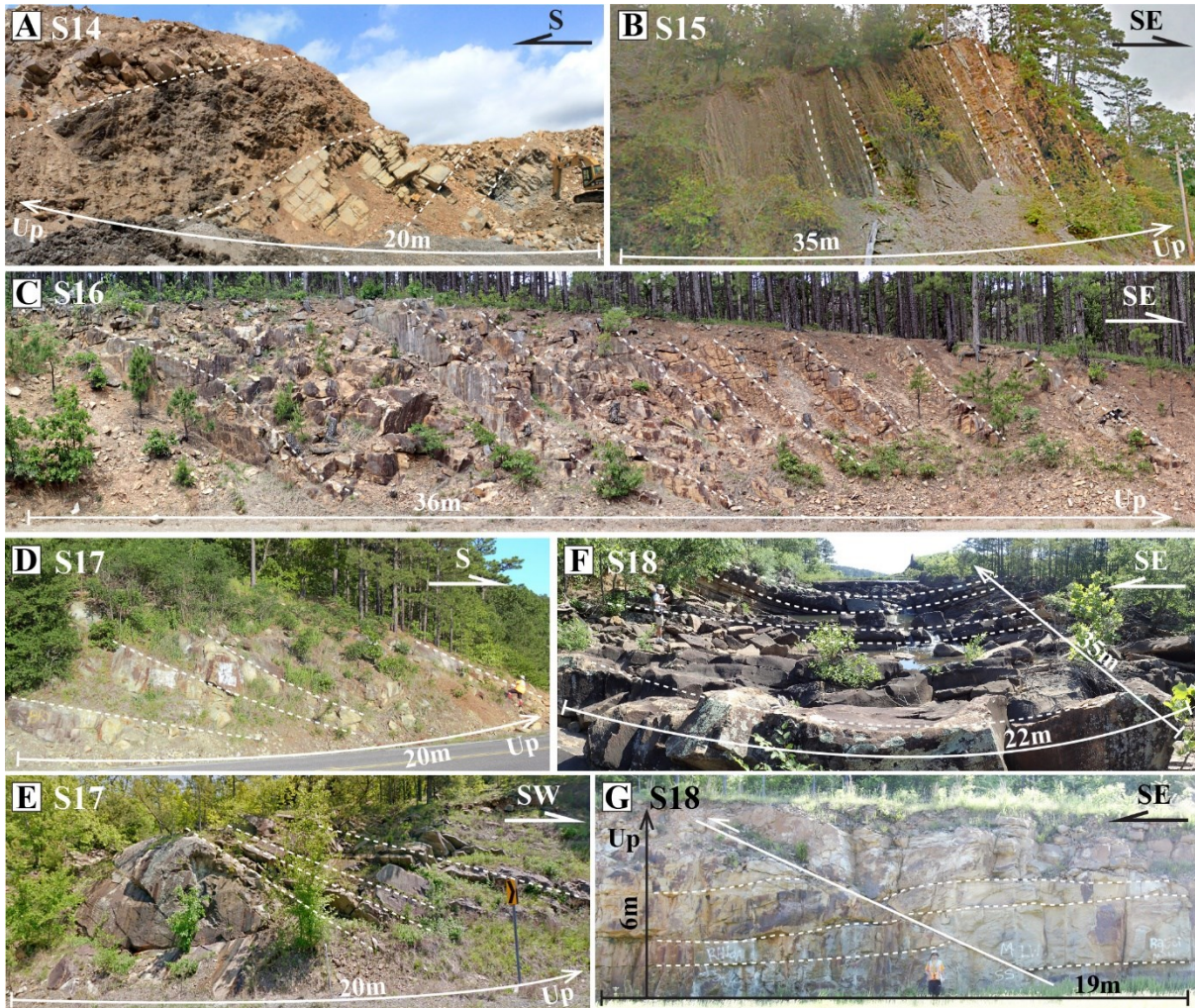


FIG. 12. – Representative outcrop photo panels of the lower Atoka formation in the wedge-top zone. A. thick-bedded, sand-rich lobes and heterolithic mudstone sheets at S14 (Antoine Quarry, Arkansas). B. sand-rich lobes and heterolithic, laminated mudstone sheets at S15 (Narrows Dam/Hinds Bluff, Arkansas). C. thick-bedded lobes at S16 (US259, Arkansas). D & E. thick-bedded, sand-rich lobes, and channel fill deposits at S17 (OK Hwy 82, Oklahoma). F. sand-rich channel fill and lobe deposits at S18 (Clayton Lake State Park, Oklahoma). G. massive, sand-rich channel fill deposits at S18 (US271, Oklahoma). Please see Table 5 for more descriptions.

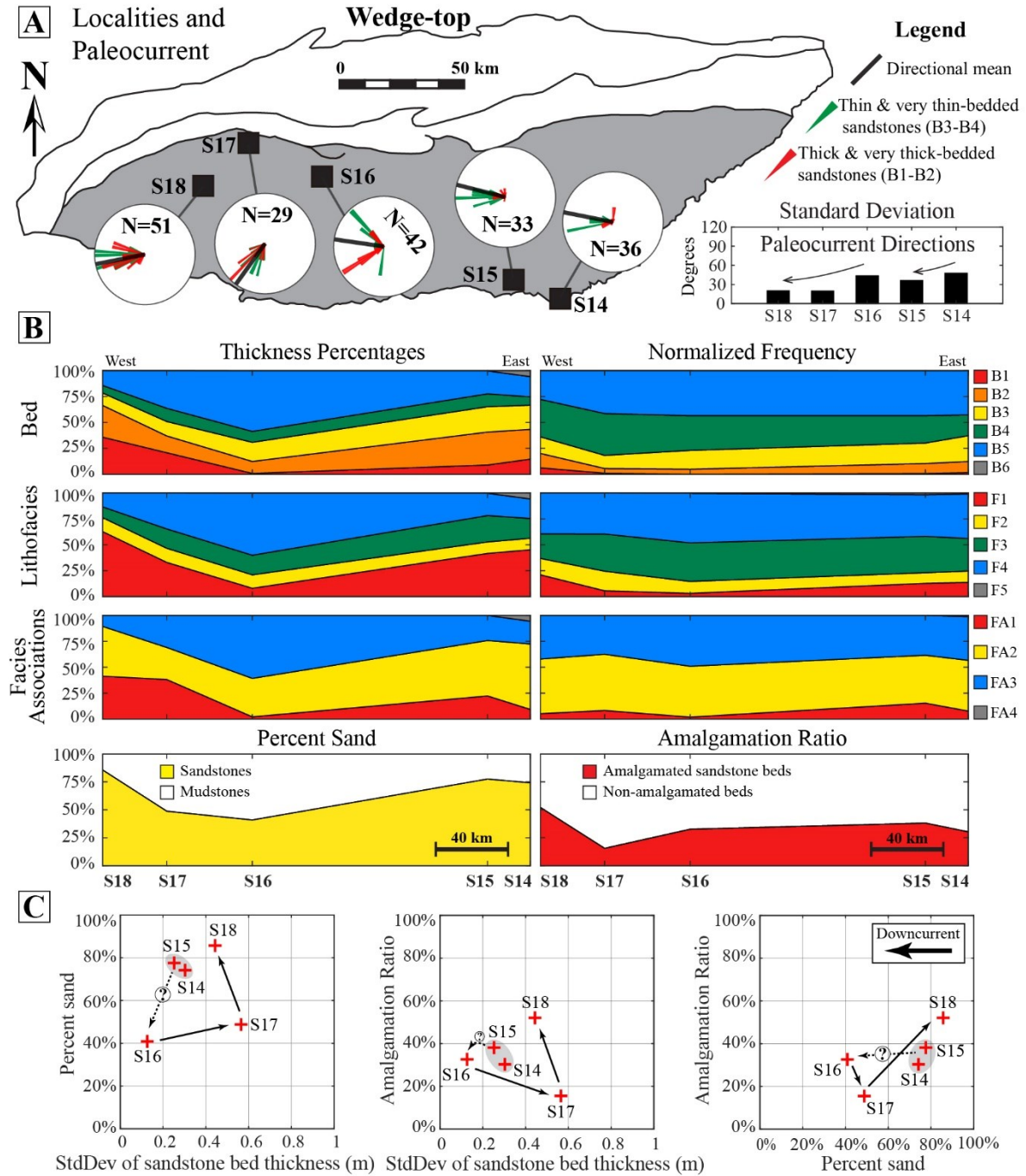


FIG. 13. – Facies distribution showing longitudinal trends in the wedge-top zone. A. all localities show primarily strike-parallel paleocurrent patterns. Standard deviations of the paleocurrent directions are low. B. area plots showing an overall decrease of sand-rich facies components from S14 to S16, and an increase from S16 to S18. The normalized frequencies are relatively stable. C. scatter plots showing no well-defined proximal-distal downcurrent trend from S14 to S18 in percent sandstone, amalgamation ratio, or variation in sandstone bed thickness.



FIG. 14. – Representative outcrop photo panels of the lower Atoka formation in the southern foreland. A. channel fill of amalgamated sandstones at S1 (Blue Mountain Dam, Arkansas). B. clay-rich, laminated mudstone sheet deposit at S1 (Blue Mountain Lake entrance, Arkansas). C & D. lobes of thin- to thick-bedded sandstones and mudstones at S2 (Atoka Reservoir, Oklahoma). Please see Table 5 for more descriptions.

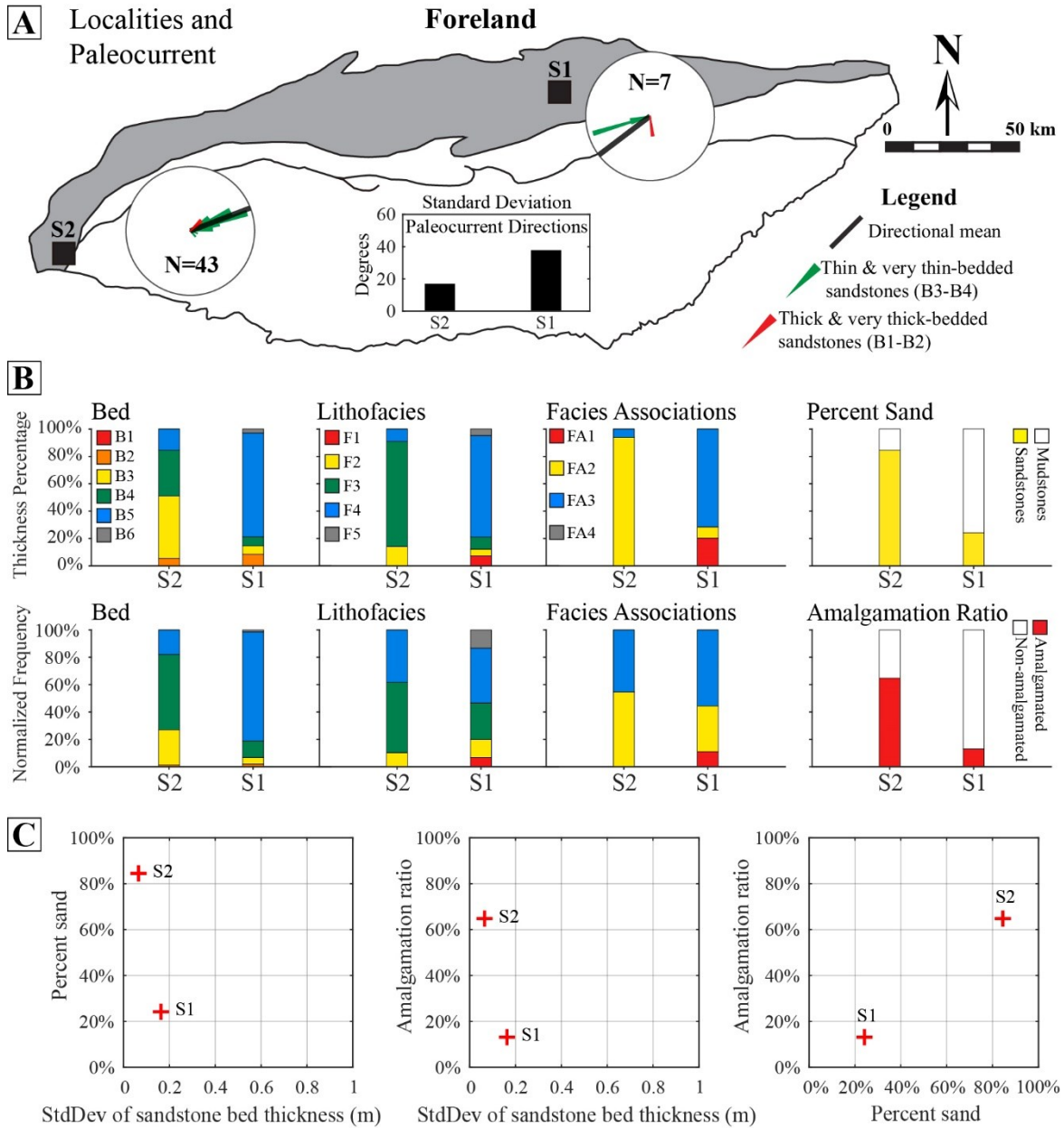


FIG. 15. – Facies contrast for the two selected composite sections in the southern and southwestern foreland. A. The contrast of paleocurrent patterns of the two localities. B. The contrast of facies compositions of the two localities. S2 is overall more sand-rich and lobe-dominated. C. Scatter plots showing that S2 is higher in percent sand, amalgamation ratio, but lower variability in sandstone thickness.

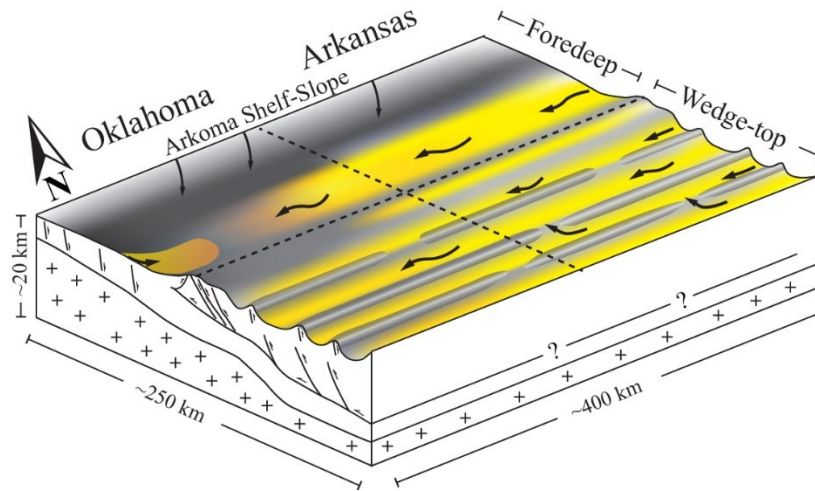


FIG. 16 Proposed conceptual depositional model of the lower Atoka formation in this study. The wedge-top shows stronger lateral topographic confinement than the foredeep. The study area is divided into four regions: proximal foredeep, distal foredeep, proximal wedge-top, and distal wedge-top. The basin is primarily sourced from the east, but also intermittently from the craton to the north and the Arbuckle Mountains to the west. The sand-rich facies components decrease rapidly from east to west in the foredeep (except in the western margin) but remain relatively stable in the wedge-top. Basin reconstruction in cross-section after Arbenz (2008).

TABLES

TABLE 1. – Summary of qualitative outcrop observations of the lower Atoka.

Zone	Area	Descriptions	Reference
Foreland	S1	mudstone olistostromes, sand dikes at Blue Mountain Dam.	Bush et al (1977, 1978)
	S2	some thick-bedded sandstone intervals near Atoka Reservoir Dam, only visible and accessible at low lake level.	This study
Foredeep	S3	common scour features in thin sections from turbidite mudstones. Silt 60-70%, sand 0-15%, clay 15-30%.	Clark et al (1999, 2000)
	S4	1. slump dominated intervals of tens of meters. 2. thick-bedded, tabular sandstones near the top of lower Atoka, Perryville.	Sprague (1985); Fulton (1985); this study
	S5	intermittent outcrops of thick-, thin-, sometimes massive sandstones and disturbed beds, vegetated.	This study
	S6	thick-bedded tabular sandstone near the top of lower Atoka, contorted ripple-laminations common, Ola Quarry.	This study
	S7	erosive, thick-bedded sandstones overlaying heterolithic mudstone interval, near the top of lower Atoka, Nimrod Lake.	This study
	S11	very thick-bedded, amalgamated, or massive sandstones south of Hodgen, OK. Paleocurrents due west.	This study
	between S11-S12	1. erosive, massive sandstones at the base. 2. Horizons of bioclasts of mollusks, clay pebbles, carbonaceous sand. 3. thick to massive sandstones at the top, planar-ripple-hummucky laminations, indicative of storm-influenced turbidite. Paleocurrents due east. basal Atoka. Eagle Gap, Arkansas, southern foreland.	Nally (2006)

TABLE 1. – Summary of qualitative outcrop observations of the lower Atoka (continued).

Zone	Area	Descriptions	Reference
Foredeep	S12	1. Johns Valley-like olistostromes in possible Atoka shale. 2. large chert block surrounded by Atoka turbidites. Both near Ti Valley, OK. 3. intermittent outcrops of thick mudstone intervals with disturbed beds, highly vegetated. 4. occasional occurrences of thick-bedded or amalgamated sandstones.	Ferguson & Suneson (1987)
	S13	thick-bedded/ amalgamated sandstones separated by long mudstone intervals. Sandstones show loading, flute casts, abundant tool marks at the base, ripple-swaley- hummocky laminations near the top, contorted bedding or truncated top, sand or mud clasts, plant debris. Some paleocurrent due south. Brushy Narrows, OK. lower-middle of Atoka Fm.	Cullen et al, Fruit et al (in Suneson et al, 1990)
Wedge-top	S14	1. slump-dominated intervals and olistostromes of sandstones near basal Atoka. 2. fragments of re-worked shallow marine invertebrate fossils	Walthall 1967); Sprague (1985); Stone et al (1981)
	S15	1. transported mold fauna of mollusks. 2. mudstone olistostromes with abundant plant debris	Bush et al (1977); Stone et al (1981)
	S16	1. shallow channel-fill sandstones. 2. abundant channel fills and MTD near basal Atoka (subsurface).	Sutherland & Manger (1979); Legg et al (1990)
	S17	brachiopod fragments in some sandstone beds, near basal Atoka	Suneson & Ferguson (1987)
	S18	intermittent outcrops of massive and very thick-bedded sandstones	This study

TABLE 2. – *Classification and characteristics of bed types.*

Lithology	Bed Type	Thickness Range	Sedimentary Structures
Sandstone Bed	B1	> 100 cm	planar stratification, basal scour and loading structures; rare mud clasts and hybrid-event-bed intervals near top of bed
	B2	30-100 cm	graded, planar stratification, occasional basal scour and loading structures
	B3	10-30 cm	planar or ripple laminations, graded bedding, flat base and rippled-top common
	B4	< 10 cm	fine ripple or planar laminations, wavy or flat
Mudstone Bed	B5	> 2 cm	fissile, finely laminated or massive
Chaotic Bed	B6	5 cm -1300 cm	contorted sandstone, mudstone, or interbedded of both, olistostromes, or reworked sand/mud clasts

TABLE 1. – *Definitions and characteristics of lithofacies used in this study.*

Code	Lithofacies Name	Typical Thickness Range (m)	Mean Percent Sand	Mean Amalgamation Ratio	Grain Size	Contacts	Sedimentary Structures	Inferred Process
F1	massive, amalgamated sandstone	1.08-4.76	99%	74%	fine - medium	Sharp and erosive base common; sharp, truncated, or gradational top	structureless or graded, sometimes ripple or planar stratified; loading structures, internal scour, mudclasts, plant debris common; trace fossils rare	rapid deposition from large magnitude, high-density turbidity currents
F2	thick-bedded sandstone with minor mudstone	0.38-1.60	95%	33%	fine	Flat base without significant erosion; flat, sometimes rippled or planar laminated top	planar or sometimes cross stratified, or weakly ripple-laminated, normal grading common; flute cast and tool marks common at the sole; loading, dewatering, and mudclasts occur occasionally; trace fossils uncommon	rapid deposition from high-density turbidity currents
F3	thin-bedded sandstone and mudstone	0.17-1.33	79%	39%	very fine - fine	Flat, non-erosive base; flat or rippled top	common planar or ripple laminations; ripples occasionally contorted; flute casts, tool marks, trace fossils common; associated mudstones silty and heterolithic	deposition from low-density turbidity currents
F4	mudstone with minor sandstone	0.06-1.97	7%	0%	silt - clay	flat, non-erosive base and top	massive, parallel- or ripple-laminated silt and clay; terrestrial plant fragments, trace fossils common on bedding planes; associated with minor very thin- and thin-bedded sandstones	deposition from dilute turbidity currents and hemipelagic fallout
F5	disturbed mudstone and sandstone	0.25-6.92	22%	13%	clay - fine	irregular base and top	contorted, chaotic, rubble bedding common; local olistostromes, sand or mud breccias	mass failure and debris flow

Note: 1. thickness ranges are 10th-90th percentiles of the thickness ranges. 2. the inferred processes are after Bouma (1962), Morris (1971), Lowe (1979), and Lowe et al (1982).

TABLE 4. – *Definitions and characteristics of facies associations in this study.*

Code	Facies Associations	Thickness (m)	Percent Sand	Amalgamation Ratio	Lithofacies Compositions	Geometry	Description	Depositional Interpretation
FA1	channel	1.03-8.14 mean: 4.00	84- 100% mean: 96%	42-100% mean: 75%	major F1, F2; minor F5, F3	channel- form, wedge, lens, or irregular	decimeters-meters of basal erosion, concentration of mudclasts near base, common scour-and-fills, some cross stratifications, and pinch-outs; occasionally filled with disturbed beds or thin-bedded sandstones	primarily distributary, shallow channels
FA2	lobe	0.46-6.37 mean: 2.72	68- 100% mean: 89%	0-89% mean: 48%	major F2, F3, some F1	tabular	flat basal contact with minor or no erosion; sandstone beds commonly graded, with well-defined Bouma Sequence; vertical trends not well-defined; may contain mudstones up to 0.4m.	lobe or basin floor fan
FA3	mudstone sheet	0.40-4.44 mean: 1.98	0-38% mean: 13%	0-5% mean: 2%	major F4, minor F3	tabular	flat, non-erosive basal and top contacts; may contain isolated thin-bedded sandstones; may be interrupted by MTD; needs to be at least 0.4m thick	interlobe, basin floor mudstone, or levee
FA4	mass transport deposit	0.63-9.71 mean: 3.35	0-68% mean: 17%	0%	major F5, minor F4	irregular	consists of one or multiple mass failure events; disturbed beds in channels not included;	mass transport deposit

Note: thickness ranges are 10th-90th percentiles of the thickness ranges.

TABLE 5. – *Descriptions and interpretations of the composite sections used in this study.*

Sec#	Description	Interpretation
S1	Lower outcrop (1): thick, fissile mudstone sheet with minor isolated sandstones. PC due west. Upper outcrop (2): heterolithic mudstone sheet, thin-bedded sandstone sheet, and slump deposits eroded and overlain by massive, amalgamated sandstone. PC due south.	Lower: slope & marginal lobe. Upper: channel and levee.
S2	Thick- & thin-bedded sandstone sheets, planar, ripple, or convoluted laminations, virtually no erosion, bioturbation common on the sole of beds. PC due northeast.	marginal lobe
S3	Thick-, thin-bedded, or amalgamated sandstone sheets and channel fills. Mudstone sheets often heterolithic, sand- or silt-rich. Muddy slumps and debrites common. Possible rafted blocks. Erosional contacts, loading structures, water escape common. Occasional cross-stratification. Paleocurrents due west. These facies characteristics can be traced >12km longitudinally.	mixed channel-lobe, proximal lobe, CTLZ?
S4	Thick-, thin-bedded, and amalgamated sandstone sheets, channel fills, heterolithic mudstone sheets, interrupted by mudstone or sandstone slumps. PC due northwest. Erosional and amalgamated contacts, loading structures, dewatering structures, trace fossils common. These facies characteristics can be traced >10km longitudinally.	mixed channel-lobe, proximal lobe
S5	East outcrop (8): thin- and thick-bedded, occasional amalgamated sandstone sheets, heterolithic mudstone sheets, interrupted by mixed sandy/muddy slumps. West outcrop (13): thin- and thick-bedded sandstone sheets, heterolithic mudstone sheets. Erosional contacts rare. Trace fossils and plant debris rare for both. PC due west.	lobe with minor channel
S6	Very thick-, thick-, and thin-bedded sandstone sheets, channel fills with massive-amalgamated sandstones, and thin, heterolithic mudstone sheets. Most beds with flat bases and tops. Loading structures, mud clasts common for thick and massive sandstones. Plant debris common, trace fossils rare. Coaly horizons. PC due west.	mixed channel-lobe, proximal lobe
S7	Mainly thin- and thick-bedded sandstone sheets and heterolithic mudstone sheets. Occurrences of massive-amalgamated sandstones increase northward (upward). Slumps rare. Planar stratification common, loading structures, mud clasts, plant debris, trace fossils rare. PC due west.	lobe with some channel,
S8	Mainly thick-bedded sandstone sheets, channel fills with massive-amalgamated sandstones, and heterolithic mudstone sheets. Sandstone beds mostly tabular, some lenticular or wedge-shaped. Loading and erosion are common at the bases of massive sandstones. Some sandstones show weak cross-stratification. Trace fossils, plant debris, mud clasts rare. PC due west for all outcrops.	mixed channel-lobe, proximal lobe
S9	Mainly thin- and thick-bedded sandstone sheets and heterolithic mudstone sheets. Loading structures, mud clasts, erosion not common. Most sandstones are tabular with flat tops and bases. Occurrences of thick-bedded sandstones increase toward the north (upwards). Trace fossils, plant debris, occur at outcrop 29. PC due west.	lobe and interlobe
S10	Mainly thin-bedded sandstone sheets and heterolithic, rhythmic mudstone sheets. Thick-bedded sandstones, slumps, erosions, mud clasts rare. Loading structures, trace fossils, sole marks, ripple and convolute laminations common. Thinning and fining upward cycles. PC due west.	marginal or distal lobe

* PC: paleocurrent.

TABLE 5. – *Descriptions and interpretations of the composite sections used in this study (continued).*

Sec#	Description	Interpretation
S11	Predominantly heterolithic and fissile mudstone sheet with isolated thin-bedded sandstone sheets, occasionally slumps. The sandstones show planar, ripple, or convoluted laminations. Thick-bedded sandstones are rare. Trace fossils and sole marks very common at the sole of sandstones. Paleocurrents due from northwest to southwest.	muddy basin floor, with some distal lobe
S12	Predominantly heterolithic and fissile mudstone sheets with isolated thin-bedded sandstones. Outcrops with some thick-bedded sandstones are also reported by Suneson & Ferguson (1987). The sandstones are often ripple-laminated with abundance trace fossils on the sole. The PC in this region are bimodal, the northern fault blocks due west while the southern fault blocks due east.	muddy basin floor, with opposing fans?
S13	Thick- and thin-bedded sandstone sheets and sand/silt-rich mudstone sheets. The sandstones are planar, or ripple laminated with abundant sole marks and bioturbation. Some sandstones show convolute laminations. Loading structures common. Erosion, amalgamation, slumps rare. PC due northeast.	storm-influence turbidite lobe?
S14	Thick-bedded and massive-amalgamated sandstone sheets, channel fills, heterolithic mudstone sheets, and some slump/ debris flow deposits. Loading structures, dewatering, erosional contacts, plant imprints, sole marks common. Trace fossils, mud clasts/pebbles occasional. Thinning- and thickening-upward cycles. PC due west, some due north.	mixed channel-lobe, proximal lobe
S15	Thick-, very thick-bedded, or massive-amalgamated sandstone sheets, channel fills, heterolithic or fissile mudstone sheets, and some muddy debrites. Erosional contacts, loading structures, sole marks common. Some plant imprints, trace fossils. PC due west, some due north.	mixed channel-lobe, proximal lobe
S16	Mixed sandstone and mudstone sheets, some debris flow deposits. SS sheets are thick- and thin-bedded sandstones, some massive-amalgamated sandstones. Tabular, planar stratified, sole marks and trace fossils common. Some convoluted laminations and loading structures. Lack of erosional contacts, plant imprints. Mudstone sheets are heterolithic or fissile, often meters thick. PC bimodal, northwest and southwest.	mixed lobe zone, axial and marginal lobe.
S17	Mixed sandstone and mudstone sheets, some channel fills. SS sheets are thick- and thin-bedded sandstones. Planar or ripple laminations, sole marks and trace fossils on thin-bedded sandstones. Some convoluted lamination, loading and erosional contacts. Channel fills are massive-amalgamated sandstones. Mudstone sheets are fissile or heterolithic. PC due southwest.	mixed channel-lobe,
S18	Characterized by massive-amalgamated or thick-bedded sandstone sheets and channel fills. Thicker sandstones show basal erosion, planar stratification, and rippled-top. Thinner sandstones show flat base and top, planar or ripple laminations. Flute casts common. Lack of trace fossils, plant imprints, mud clasts, soft-sediment deformation. Mudstone sheets are heterolithic, rich in sand and silt. PC due west.	mixed channel-lobe, proximal lobe.

* PC: paleocurrent.

SUPPLEMENTARY MATERIAL

TABLE – Outcrop localities of the lower Atoka formation.

FIGURES – Measured sections of the lower Atoka formation.